Introduction to Quantum Chromodynamics

Michal Šumbera

Nuclear Physics Institute ASCR, Prague

November 3, 2009

Elements of the parton model

1. Kinematics
2. Dynamics
3. Cross–sections of virtual photons
4. Electrons as tools for investigating nuclear structure
5. What does the deep inelastic scattering of electrons tell us about the structure of nucleons?
6. Emergence of the parton model
7. Parton distribution functions and their basic properties
8. Parton model in neutrino interactions
9. Polarized nucleon structure functions
10. Space–time picture of DIS and hadronization
11. Parton model in other processes
12. Electron-positron annihilations into hadrons
13. Drell-Yan production of heavy dilepton pairs
14. Exercises

Literature

Our discussion is based on

Quarks, partons and Quantum Chromodynamics
by Jiří Chýla
Available at http://www-hep.fzu.cz/ chyla/lectures/text.pdf

Additional material comes from

Quantum Mechanics – Non-Relativistic Theory
by L. D. Landau and E. M. Lifshitz
Pergamon Press 1976 (Third edition)

Kinematics

- For definiteness, all relations will be written for lepton-proton scattering

$$\ell(k) + \text{proton}(P) \to \ell'(k') + X; \quad \ell, \ell' = e, \mu, \nu_e \nu_\mu, \tag{1}$$

where X denotes *any* final state allowed by conservation laws and the letters in brackets stand for four–momenta of the corresponding particles.

- A special case of (1) is the elastic lepton-nucleon scattering, when X=proton and $\ell = \ell'$.

- There are two types of lepton-nucleon scattering processes, called
  - **neutral current** processes, when $\ell' = \ell$. These processes can be mediated by the exchange of either the photon or the (neutral) intermediate vector boson Z, but in the kinematical range we shall be interested in, the latter contribution can be safely neglected.
  - **charged current** processes, when the electric charges of the initial and final leptons ℓ, ℓ' differ by one unit. These processes are mediated by the exchange of charged intermediate vector bosons $W^\pm$.

Kinematics

- The selection of variables describing (1) is a matter of convention, but the following set is commonly used (see Fig. 1)[1]
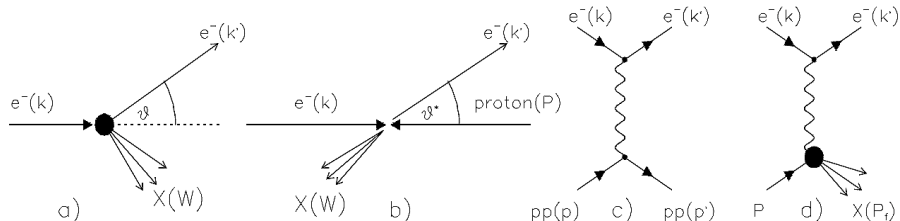

Figure 1: The DIS scattering in laboratory (a) and CMS (b) frames and the lowest order Feynman diagram describing the scattering on a pointlike proton, denoted "pp" (c).

Kinematics

$$S \equiv (k + P)^2 = M_p^2 + 2kP = M_p(2E_{lab} + M_p), \tag{2}$$

$$Q^2 \equiv -q^2 \equiv -(k - k')^2 = 2kk' = 4EE' \sin^2(\vartheta/2), \tag{3}$$

$$y \equiv \frac{qP}{kP} = \frac{E_{lab} - E'_{lab}}{E_{lab}} = \frac{\nu}{E_{lab}} = \left(\frac{s - M_p^2}{s}\right)\frac{1 - \cos\vartheta^*}{2}, \tag{4}$$

$$x \equiv \frac{Q^2}{2Pq} = \frac{Q^2}{2M_p\nu} = \frac{Q^2}{Q^2 + W^2 - M_p^2}, \tag{5}$$

$$W^2 \equiv (q + P)^2 = \frac{Q^2(1 - x)}{x} + M_p^2. \tag{6}$$

- W is invariant mass of the hadronic system X, produced by the absorption of the exchanged photon by the target nucleon (missing mass).
- N.B. Only k', k and P are needed to evaluate x, y and Q^2.
- The last equality in (3) holds in *any* reference system.
- All five quantities defined above are relativistic *invariants*.

---

(1) In the following m will denote generic lepton masses and M_p the proton mass. In most cases m will be neglected, but the latter kept.

Kinematics

- In the laboratory frame (p is at rest) they can be expressed by means of the scattering angle ϑ_{lab} and the energies E_{lab}, E'_{lab} of the primary and scattered lepton:

$$E'_{lab} = \frac{E_{lab} - (W^2 - M_p^2)/2M_p}{1 + E_{lab}\left(1 - \cos\vartheta_{lab}\right)/M_p}. \tag{7}$$

- The variable S specifies the initial state of the colliding electron and proton, while x, y, q^2, ϑ and E'_{lab}, describe, for given S and the azimuthal angle ϕ, the final state of an electron in (1).

- As, however, only two of them are independent, one can thus choose any of the pairs (x, y), (x, q^2), (y, q^2), or $(E'_{lab}, \vartheta_{lab})$ to uniquely specify the state of the scattered electron provided the colliding particles are *unpolarized* [2]. Unless mentioned otherwise, this will always be assumed.

- In modern notation the pairs (x, y) or (x, Q^2) are most often used to write down the cross–section of (1).

---

(2) In the case of the scattering of unpolarized particles the trivial dependence on ϕ is integrated over..

Kinematics

- For given total CMS energy squared S, these variables are related:

$$Q^2 = xy(2kP) = xy\left(S - M_p^2\right). \tag{8}$$

- In (unpolarized) elastic e+p scattering final state is described, beside azimuthal angle, by one independent variable only, for which one can take any of the following Q^2, y, ϑ or E'_{lab}. In the following the scattering angle ϑ_{lab} or $y \doteq (1 - \cos\vartheta^*)/2$ will usually be used for this purpose [3]

- For elastic scattering we find that x and W^2 are fixed by kinematics, $x = 1$ and $W^2 = M_p^2$, and the relation (7) implies that ϑ and E'_{lab} are related

$$E'_{lab} = \frac{E_{lab}}{1 + E_{lab}\left(1 - \cos\vartheta_{lab}\right)/M_p}. \tag{9}$$

- The term "deep inelastic scattering" means that both invariants Q^2 and Pq are large with respect to M_p $\quad Q^2 = -q^2 \gg M_p^2; \quad \nu \gg M_p. \tag{10}$

- The so called **Bjorken limit** corresponds to the idealized case when $Q^2 \to \infty, Pq \to \infty$ but the ratio $x \equiv Q^2/2Pq$ remains finite.

---

(3) Quantities in the c.m.s. will be labeled by $*$ and the symbol $\doteq$ will denote approximate equality, neglecting the mass of the proton or target parton. Recall that the mass of an electron is always neglected.

Elastic collisions between fast electrons and atoms

- If the velocity of the incident electron is large compared with those of the atomic electrons $\Rightarrow$ can be treated by means of the Born approximation (KM2, p156).

$$f(\mathbf{k} \to \mathbf{k}') = -m(2\pi)^2 \hbar \langle \mathbf{k} \mid V \mid \mathbf{k}' \rangle = -\frac{m}{2\pi\hbar^2} \int d^3 r e^{-i\mathbf{q}\cdot\mathbf{r}} V(r), \quad \mathbf{q} = \mathbf{k}' - \mathbf{k} \tag{11}$$

- $m_e \ll m_A \Rightarrow$ c.m.s. coincides with rest system of the atom. Then $\mathbf{k}$ and $\mathbf{k}'$ in formula (11) denote the momenta of the electron before and after the collision, m the mass of the electron, and the angle θ is the same as the angle of deviation ϑ of the electron.

- In a collision with an atom $V(r)$ corresponds to the potential energy of the interaction of the electron with the atom, averaged with respect to the wave function of the latter. It is $e\phi(r)$, where $\phi(r)$ is the potential of the field at the point r due to the mean distribution of charges in the atom:

$$\Delta\phi = -4\pi\rho(r) \tag{12}$$

where $\rho(r)$ is density of the charge distribution in the atom.

Elastic collisions between fast electrons and atoms

- Solution via Fourier transform is:

$$\int \phi e^{-i\mathbf{q}\cdot\mathbf{r}} d^3 r = \frac{4\pi}{q^2} \int \rho e^{-i\mathbf{q}\cdot\mathbf{r}} d\mathbf{r} \tag{13}$$

- Since $\rho(r)$ consists of the electron charges and the charge on the nucleus:

$$\rho(r) = -en(r) + Ze\delta(r) \tag{14}$$

(13) can be rewritten as:

$$\int \phi e^{-i\mathbf{q}\cdot\mathbf{r}} d^3 r = \frac{4\pi}{q^2} \left[Z - F(q) \right] \tag{15}$$

where we have introduced *atomic form factor $F(q)$*

$$F(q) = \int n e^{-i\mathbf{q}\cdot\mathbf{r}} d^3 r \tag{16}$$

- Finally

$$\frac{d\sigma}{d\Omega} = |f(\mathbf{k} \rightarrow \mathbf{k}')|^2 = \frac{4m^2 e^4}{\hbar^4 q^4} \left[Z - F(q) \right]^2, \quad q = \frac{2mv}{\hbar} sin\frac{\vartheta}{2} \tag{17}$$

Elastic collisions between fast electrons and atoms

- Consider $qa_0 \ll 1$, where $a_0 \sim r_A$. Small ϑ correspond to small q:
  $\vartheta \ll v_0/v$, where $v_0 \sim \hbar/ma_0 \sim v_e^A$. Expanding $F(q)$ in powers of q the
  zero-order term is $\int n d\mathbf{r} = Z$, i.e. number of electrons in the atom.
  First-order term $\int \mathbf{r} n(r) d\mathbf{r}$ (average value of the dipole moment) is zero and
  up to second-order term we have:

$$Z - F(q) = \frac{q^2}{6} \int r^2 n d^3 r \Rightarrow \frac{d\sigma}{d\Omega} = \left| \frac{me^2}{2\hbar^2} \int n r^2 d^3 r \right|^2 \qquad (18)$$

  Thus, *in the range of small angles, the cross-section is independent of the
  scattering angle*, and is given by the mean square distance of the atomic
  electrons from the nucleus.

- In the opposite limit $qa_0 \gg 1$, $\vartheta \gg v_0/v$ exponential $e^{-i\mathbf{q}\cdot\mathbf{r}}$ becomes rapidly
  oscillating function bringing integral (16) close to zero. Consequently, in
  expression (15) we can neglect the atomic form factor F(q) in comparison
  with Z, so that:

$$\frac{d\sigma}{d\Omega} = \left(\frac{Ze^2}{2mv^2} \right)^2 \frac{1}{\sin^4 \frac{\vartheta}{2}} \qquad (19)$$

  i.e. *Rutherford formula* for elastic scattering of electron on the atomic
  nucleus.

Dynamics

- The basic quantity describing the general scattering process

$$1 + 2 \to 3 + 4 + \cdots n \tag{20}$$

is $d\sigma = \dfrac{(2\pi)^4}{\mid \vec{v}_1 - \vec{v}_2 \mid} \dfrac{1}{2E_1} \dfrac{1}{2E_2} \left| M_{if} \right|^2 \prod_{i=3}^{n} \dfrac{d\vec{p}_i}{(2\pi)^3 2E_i} \delta^4(p_1 + p_2 - \sum_{i=3}^{n} p_i)\, SF,$ (21)

where E_i is the energy of particle i with velocity $\vec{v}_i$ (in units of c), M_{if} is invariant amplitude of (20), corresponding to the normalization of incoming and outgoing one–particle states $\mid E, \vec{p} \rangle$ of energy E and momentum $\vec{p}$:

$$\langle E', \vec{p}\,' \mid E, \vec{p} \rangle = (2\pi)^3 2E \delta^3(\vec{p} - \vec{p}\,') \tag{22}$$

and the statistical factor

$$SF \equiv \prod_i \frac{1}{n_i!} \tag{23}$$

applies to n_i identical particles of type i in the final state.

- N.B. (21) assumes that the particles 1, 2 collide head on, otherwise more general expression would replace $\mid \vec{v}_1 - \vec{v}_2 \mid 2E_1 2E_2$, which is invariant with respect to Lorentz boosts along the direction of these colliding particles.

Dynamics

Elastic scattering of electrons on pointlike proton

- Similarly to Rutherford experiment, we have to know elastic lepton-proton cross section (21) for the case of *pointlike* proton with momentum p and mass M.

- In the lowest order of *pQED* we have photon exchange diagram of Fig. 1c:

$$\left| \overline{M_{if}} \right|^2 = \frac{1}{4} \sum_{spins} \left| [\overline{u}(k', s_4)\gamma_\mu u(k, s_2)] \, e^2 \frac{-ig^{\mu\nu}}{q^2} [\overline{u}(p', s_3)\gamma_\nu u(p, s_1)] \right|^2 . \quad (24)$$

$u, \overline{u}$ are the usual Dirac bispinors, satisfying the free particle Dirac equations

$$(\not{p} - m)u(p) = 0; \quad \overline{u}(p)(\not{p} - m) = 0 \quad \text{where} \quad \not{p} \equiv \gamma^\mu p_\mu \quad (25)$$

and are normalized as

$$\overline{u}(p)u(p) = -\overline{v}(p)v(p) = 2m; \quad u^+(p)u(p) = v^+(p)v(p) = 2E \quad (26)$$

and the photon propagator is taken in the Feynman gauge. In (24) we have summed over the spins s_3, s_4 of the final and averaged over the spins s_1, s_2 of the initial fermions reads

Elastic scattering of electrons on pointlike proton

- (24) can be written as the contraction of two tensors (*TP172*)

$$\left|\overline{\mathrm{M_{if}}}\right|^2 = \frac{e^4}{Q^4} L^{(1)\mu\nu} L^{(2)}_{\mu\nu}, \tag{27}$$

where

$$L^{(1)}_{\mu\nu} \equiv \frac{1}{2}\mathrm{Tr}\left[(\not{k}' + m)\gamma^\mu(\not{k} + m)\gamma^\nu\right] = 2\left[k^\mu k'^\nu + k^\nu k'^\mu - g^{\mu\nu}(kk' - m^2)\right] \tag{28}$$

describes upper, electron vertex of Fig. 1c. Similarly, $L^{(2)}_{\mu\nu}$ describes lower, proton, vertex and is given by (28) with $k \to p$, $k' \to p'$, $m \to M$.

- Carrying the contraction as indicated in (27) we get

$$
\begin{aligned}
L^{(1)\mu\nu} L^{(2)}_{\mu\nu} &= 8[\underbrace{(k'p')}_{kp}(kp) + \underbrace{(k'p)}_{k'p}(kp') - M^2\underbrace{(kk')}_{-q^2/2} - \underbrace{m^2(pp') + 2m^2M^2}_{\text{neglected}}] \\
&= 8(kp)^2\left[1 + \left(\frac{k'p}{kp}\right)^2 + \frac{M^2q^2}{2(kp)^2}\right] \tag{29} \\
&= 8(kp)^2\left[1 + (1-y)^2 - \frac{M^2y}{kp}\right] \xrightarrow[kp\to\infty]{} 8(kp)^2\left[1 + (1-y)^2\right],
\end{aligned}
$$

where $(kp) = (s - M^2)/2$ specifies the primary energy of the colliding particles and $(k'p)/(kp) = 1 - y$ describes the final state.

Elastic scattering of electrons on pointlike proton

- For $s \to \infty$ (30) takes particularly simple form. In the CMS of the colliding particles we have

$$y \equiv \frac{qp}{kp} = \left(\frac{s - M^2}{s}\right) \frac{1 - \cos \vartheta^*}{2} \doteq \frac{1 - \cos \vartheta^*}{2}$$

$$\Rightarrow \mathrm{d}y = -\left(\frac{s - M^2}{2s}\right) \mathrm{d}\cos\vartheta^* \doteq -\frac{\mathrm{d}\cos\vartheta^*}{2}, \tag{30}$$

the integral over the phase space elements gives

$$\int\int \frac{\mathrm{d}^3 \vec{p}\,'}{2E_{p'}} \frac{\mathrm{d}^3 \vec{k}\,'}{2E_{k'}} \delta^4(k + p - k' - p') = \int \left(\frac{s - M^2}{8s}\right) \mathrm{d}\Omega \doteq \frac{1}{8}\int \mathrm{d}\Omega \tag{31}$$

and the flux factor reduces to

$$\frac{1}{2E_k} \frac{1}{2E_p} \frac{1}{\mid v_1 - v_2 \mid} = \frac{1}{2(s - M^2)}, \tag{32}$$

where we have retained the nonzero mass M of the target "pointlike proton".

Elastic scattering of electrons on pointlike proton

- Substituting the above expressions into (21), integrating over ϕ and replacing $\mathrm{d}\cos\vartheta^*$ with $\mathrm{d}y$ using (30) we finally get

$$\frac{\mathrm{d}\sigma}{\mathrm{d}y} = \frac{2\pi\alpha^2(2kp)}{Q^4}\left[1 + (1-y)^2 - \frac{M^2 y}{kp}\right] \Rightarrow \frac{\mathrm{d}\sigma}{\mathrm{d}Q^2} = \frac{2\pi\alpha^2}{Q^4}\left[1 + (1-y)^2 - \frac{M^2 y}{kp}\right], \tag{33}$$

where we have used the fact that $Q^2 = y2kp$.

- Carrying out the same reduction in the laboratory frame yields

$$L_{(1)}^{\mu\nu}L_{\mu\nu}^{(2)} = 16EE'M^2\left[\cos^2\frac{\vartheta_{lab}}{2} - \frac{q^2}{2M^2}\sin^2\frac{\vartheta_{lab}}{2}\right] \Rightarrow \tag{34}$$

$$\frac{\mathrm{d}\sigma}{\mathrm{d}\Omega_{lab}} = \frac{\alpha^2\cos^2(\vartheta_{lab}/2)}{4E^2\sin^4(\vartheta_{lab}/2)}\frac{E'}{E}\left[1 + \frac{Q^2}{2M^2}\tan^2\frac{\vartheta_{lab}}{2}\right] \underset{M\to\infty}{\longrightarrow} \frac{\alpha^2\cos^2(\vartheta_{lab}/2)}{4E^2\sin^4(\vartheta_{lab}/2)} = \sigma_{\mathrm{Mott}} \tag{35}$$

where σ_{Mott} is differential cross–section corresponding to scattering of a spinless particle off an infinitely heavy proton and the factor $E'/E = 1 - Q^2/2ME < 1$ takes into account the recoil.

N.B. Apart from the presence of $\cos^2(\vartheta/2)$, which is characteristic of spin 1/2 fermion, the Mott cross section represents relativistic generalization of the Rutherford formula.

Elastic scattering of electrons on pointlike zero spin boson

- Feynman rules lead to the following simple expression for the vertex boson-γ-boson in the notation as in Fig. 1: $-ie(p + p')^{\mu}$. The tensor $L_{\mu\nu}^{(2)}$ is then trivial and we get

$$L^{(1)\mu\nu} L_{\mu\nu}^{(2)} = 8(kp)^2 \left[2(1-y) - \frac{M^2 y}{kp} \right]. \qquad (36)$$

- Both of the above results can be written in a single compact form

$$\frac{\mathrm{d}\sigma}{\mathrm{d}y} = \frac{4\pi\alpha^2(2kp)}{Q^4} \left[(1-y) + \varepsilon \frac{y^2}{2} - \frac{M^2 y}{2kp} \right], \qquad (37)$$

or equivalently

$$\frac{\mathrm{d}\sigma}{\mathrm{d}Q^2} = \frac{4\pi\alpha^2}{Q^4} \left[(1-y) + \varepsilon \frac{y^2}{2} - \frac{M^2 y}{2kp} \right] \underset{s\to\infty}{\Longrightarrow} \frac{4\pi\alpha^2}{Q^4}, \qquad (38)$$

where

- $\varepsilon = 1$ for pointlike fermion with spin 1/2,
- $\varepsilon = 0$ for pointlike boson with spin 0.

- *To see a difference between the scattering on fermions and bosons requires therefore large y, i.e. large angle scattering.*

Elastic scattering of electrons on real proton

(TP p.178)

- Strong interactions modify the pointlike coupling $\bar{u}(p')[\mathrm{i}e\gamma^\mu]u(p)$ which has to be replaced with a structure, compatible with gauge and Lorentz invariance and parity conservation[1]

$$\bar{u}(p') \left[F_1(Q^2)\gamma^\mu + \kappa \frac{F_2(Q^2)}{2M_p}\mathrm{i}\sigma^{\mu\nu}q_\nu \right] u(p); \;\; \sigma^{\mu\nu} \equiv \frac{\mathrm{i}}{2}\left[\gamma^\mu\gamma^\nu - \gamma^\nu\gamma^\mu, \right] \;\; (39)$$

where $F_1(Q^2), F_2(Q^2)$ are the **elastic electromagnetic formfactors** of the proton and κ is a number, conveniently introduced in order to allow us to set $F_2(0) = 1$.

- N.B. No such parameter is needed in front of F_1 as gauge invariance implies $F_1(0) = 1$. Moreover, it is an interesting exercise in the nonrelativistic reduction of the Dirac equation to show that κ gives just the **anomalous magnetic moment** of the proton (i.e. 1.79).

(1) See next subsection for the derivation in the case of a more complicated inelastic scattering.

Elastic scattering of electrons on real proton

- The evaluation of the differential cross section using (39) is straightforward but tedious. The result

$$\frac{\mathrm{d}\sigma}{\mathrm{d}\Omega_{lab}} = \sigma_{\mathrm{Mott}} \frac{E'}{E} \left\{ F_1^2(Q^2) + \frac{Q^2}{4M_p^2} \left[2\tan^2\frac{\vartheta_{lab}}{2}\left(F_1(Q^2) + \kappa F_2(Q^2)\right)^2 + \kappa^2 F_2^2(Q^2) \right] \right.$$

(40)

to be compared to (35), was derived first by Rosenbluth in 1950.

- N.B. The pointlike "Dirac proton" corresponding to $F_1 = 1, \kappa = 0$, includes the interaction of pointlike magnetic moment equal to $\mu_p = 1$.

- Setting $F_1(Q^2) = F_2(Q^2) = 1, \kappa = 1.793$ defines the pointlike proton with anomalous magnetic moment. For the real proton the formfactors F_i are steeply falling functions of Q^2.

Elastic scattering of electrons on real proton

- Instead of F_1, F_2 it is convenient to introduce the **electric and magnetic** formfactors

$$G_E(Q^2) \equiv F_1(Q^2) - \frac{Q^2}{4M_p^2}\kappa F_2(Q^2) \Rightarrow G_E(0) = 1, \qquad (41)$$

$$G_M(Q^2) \equiv F_1(Q^2) + \kappa F_2(Q^2) \quad \Rightarrow \quad G_M(0) = 1 + \kappa = \mu_p. \qquad (42)$$

In Fig. 6a the ratio G_M/μ_p is plotted as a function of Q^2 and fitted to the dipole formula, which implies that at large Q^2, $G_M \propto 1/Q^4$! Similarly for $G_E(Q^2)$. In terms of these new formfactors ($\tau \equiv Q^2/4M_p^2$)

$$\frac{d\sigma}{d\Omega_{lab}} = \sigma_{\text{Mott}} \frac{E'}{E} \left[\frac{G_E^2 + \tau G_M^2}{1 + \tau} + 2\tau G_M^2 \tan^2(\vartheta_{lab}/2) \right]. \qquad (43)$$

Deep inelastic scattering of electrons on nucleons

- In inelastic scattering of *unpolarized* electrons on *unpolarized* protons there are *two* independent variables which uniquely specify final state of the scattered electron.
- Basic quantity of interest is then the double differential cross–section $\mathrm{d}\sigma/\mathrm{d}y\mathrm{d}x$. For electromagnetic interactions its general form reads, written in three equivalent ways, which differ by the choice of two independent variables on which the cross section depends

$$\frac{\mathrm{d}\sigma}{\mathrm{d}E'\mathrm{d}\Omega_{lab}} = \sigma_{\mathrm{Mott}} \frac{1}{M} \left[W_2(x, Q^2) + 2W_1(x, Q^2)\tan^2\frac{\vartheta}{2} \right]. \qquad (44)$$

$$\frac{\mathrm{d}\sigma}{\mathrm{d}x\mathrm{d}y} = \frac{4\pi\alpha^2(2kP)}{Q^4} \left[\left(1 - y - \frac{M_p^2 xy}{S}\right) F_2(x, Q^2) + \frac{1}{2}y^2 2xF_1(x, Q^2) \right], \quad (45)$$

$$\frac{\mathrm{d}\sigma}{\mathrm{d}x\mathrm{d}Q^2} = \frac{4\pi\alpha^2}{Q^4} \left[\left(1 - y - \frac{M_p^2 xy}{S}\right) \frac{F_2(x, Q^2)}{x} + \frac{1}{2}y^2 2F_1(x, Q^2) \right] \xrightarrow[S\to\infty]{} \frac{4\pi\alpha^2}{Q^4} \frac{F_2(x, Q^2)}{x},$$

$$\qquad (46)$$

where $S \equiv (k + P)^2$ is the square of the total CMS energy. Since $Q^2 = 2(kP)xy \Rightarrow$ the limit in the last expression follows from the fact that for fixed x and Q^2 the limit $s \to \infty$ implies $y \to 0$.

- Unknown functions $F_i(x, Q^2)$, or equivalently, $W_i(x, Q^2)$, are called **inelastic electromagnetic formfactors** or **structure functions** of the proton.

Deep inelastic scattering of electrons on nucleons

The form of (45) follows from four fundamental properties of electromagnetic interactions: Lorentz invariance, unitarity, gauge invariance and parity conservation. Its derivation proceeds in several steps.

1. tensor $L_{\mu\nu}^{(2)}$ associated in the case of elastic scattering on a pointlike proton with the lower vertex in Fig. 1d, will be replaced with the general Lorentz tensor that can be formed out of the momenta* P, q and basic tensors of rank two, i.e. symmetric metric tensor $g^{\mu\nu}$ and totally antisymmetric Levi–Civita pseudotensor $\epsilon_{\mu\nu\alpha\beta}$:

$$W_{\mu\nu}(P, q) = -W_1 g_{\mu\nu} + W_2 \frac{P_\mu P_\nu}{M_P^2} + i W_3 \epsilon_{\mu\nu\alpha\beta} P^\alpha q^\beta \qquad (47)$$
$$+ W_4 q_\mu q_\nu + W_5 \left(P_\mu q_\nu + P_\nu q_\mu \right) + i W_6 \left(P_\mu q_\nu - P_\nu q_\mu \right).$$

$W_i(P, q)$ are unknown functions of P and q which depend on proton internal structure. i in front of W_3 and W_6 assures hermiticity of the tensor $W_{\mu\nu}$, i.e. $W_{\mu\nu} = W_{\nu\mu}^*$, i.e. all $W_i(P, q)$ are *real functions*.

(*) For scattering of unpolarized leptons on unpolarized nucleons there are no other four-momenta available. In the case of polarized particles the general decomposition of $W_{\mu\nu}$ includes also structures containing their polarization vectors.

Deep inelastic scattering of electrons on nucleons

- Not all of $W_i(P, q)$ are, however, independent. Parity conservation requires $W_3(P, q) = 0$ and gauge invariance, expressed as the condition

$$q^\mu W_{\mu\nu}(P, q) = \underbrace{\left[-W_1 + W_4 q^2 + W_5(Pq) \right]}_{=0} q_\nu +$$

$$\underbrace{\left[W_2 \frac{Pq}{M_\rho^2} + W_5 q^2 \right]}_{=0} P_\nu + \underbrace{\mathrm{i} W_6 \left[(Pq)q_\nu - q^2 P_\nu \right]}_{\mathrm{imaginary} \Rightarrow W_6 = 0} = 0 \tag{48}$$

leads to three relations: $W_6 = 0$ and

$$W_5(P, q) = -W_2(P, q) \frac{Pq}{q^2 M_\rho^2}, \tag{49}$$

$$W_4(P, q) = W_1(P, q) \frac{1}{q^2} + W_2(P, q) \frac{(Pq)^2}{q^4 M_\rho^2}. \tag{50}$$

- Out of the original six functions W_i only two are thus independent.

Deep inelastic scattering of electrons on nucleons

- In terms of W_1, W_2 eq. (48) reads

$$W_{\mu\nu}(P,q) = -W_1(P,q)\left(g_{\mu\nu} - \frac{q_\mu q_\nu}{q^2}\right) + \frac{W_2(P,q)}{M_p^2}\left(P_\mu - \frac{Pq}{q^2}q_\mu\right)\left(P_\nu - \frac{Pq}{q^2}q_\nu\right).$$
(51)

- Dropping terms to q^μ or q^ν, which vanish after contraction with the leptonic tensor $L^{\mu\nu}(k,k')$, due to its transversality (i.e. $q^\mu L_{\mu\nu} = 0$), we get:

$$W_{\mu\nu}(P,q) = -W_1(P,q)g_{\mu\nu} + W_2(P,q)\frac{P_\mu P_\nu}{M_p^2}.$$
(52)

- Performing contraction $L_{\mu\nu}W^{\mu\nu}$ and neglecting m but keeping M_p

$$L^{\mu\nu}(k,k')W_{\mu\nu}(P,q) = 2\left(k^\mu k'^\nu + k^\nu k'^\mu - g^{\mu\nu}(kk')\right)\left(-W_1 g_{\mu\nu} + W_2\frac{P_\mu P_\nu}{M^2}\right)$$
(53)

we find, after some straightforward algebra and using basic kinematics,

$$L^{\mu\nu}W_{\mu\nu} = \frac{4(kP)}{y}\left[\frac{\nu}{M_p}W_2\left(1 - y - \frac{M_p^2 x^2 y^2}{Q^2}\right) + 2xW_1\frac{y^2}{2}\right].$$
(54)

Deep inelastic scattering of electrons on nucleons

- Instead of W_1, W_2 it is common to introduce another pair of functions

$$F_1 \equiv W_1, \qquad F_2 \equiv \frac{\nu}{M} W_2, \tag{55}$$

in term of which (54) reads

$$L^{\mu\nu} W_{\mu\nu} = \frac{4(kP)}{y} \left[F_2(x, Q^2) \left(1 - y - \frac{M_p^2 x^2 y^2}{Q^2} \right) + 2x F_1(x, Q^2) \frac{y^2}{2} \right] \tag{56}$$

- Inserting (56) into the general expression (21) for the corresponding cross–section and working out the differential $\mathrm{d}^3 k'$ in terms of $\mathrm{d}x \mathrm{d}y$ we finally arrive at (45).

- N.B. In elastic scattering $x = 1$ by kinematics $\Rightarrow$ relations between elastic and inelastic formfactors:

$$F_2^{\mathrm{inel}}(x = 1, Q^2) = (F_1^{\mathrm{el}}(Q^2))^2 + \frac{\kappa^2 Q^2}{4 M_p^2} \left(F_2^{\mathrm{el}}(Q^2) \right)^2, \tag{57}$$

$$2 F_1^{\mathrm{inel}}(x = 1, Q^2) = \left(F_1^{\mathrm{el}}(Q^2) + \kappa F_2^{\mathrm{el}}(Q^2) \right)^2, \tag{58}$$

Cross–sections of virtual photons

- W_1, W_2 have interpretation in terms of the total cross–sections $\sigma(\gamma^* p)$ of the "collision" between the virtual photon and the proton in the lower vertex of Fig. 1d with $W = \sqrt{Q^2(1-x)/x}$ playing the role of the total cms and Q^2 being the mass squared of incoming photon.

- While real photons exist only in 2 spin states (spin parallel or antiparallel to its momentum), corresponding to two polarization four-vectors ϵ_μ, virtual photons exist altogether in *four independent* spin states, described by polarization vectors $\epsilon_\mu^{(i)}$, $i = 1, 2, 3, 4$.

- Any treatment of photons, real or virtual, requires the selection of a particular **gauge**, which leads to additional condition on the polarization four-vectors ϵ_μ. In the so called Lorentz gauge this condition implies $\epsilon(q)q = 0$. There are three independent polarization vectors, which satisfy this *gauge fixing condition*. Assuming $\vec{q}$ to point in the "third" direction and denoting $q = (q_0, q_1, q_2, q_3)$ they can be chosen as the following real vectors:

$$\epsilon_{\mathrm{T}}^{(1)} = (0, 1, 0, 0); \quad \epsilon_{\mathrm{T}}^{(2)} = (0, 0, 1, 0); \quad \epsilon_{\mathrm{L}} = \frac{1}{\sqrt{Q^2}}(q_3, 0, 0, q_0). \tag{59}$$

Cross–sections of virtual photons

- Total cross section of a collision of the virtual photon of momentum q and polarization vector $\epsilon_\mu = (\epsilon_0, \vec{\epsilon})$ with the proton at rest (i.e. with $P = (M, 0, 0, 0)$) is given as:

$$\sigma(\gamma^* p; S) = C \epsilon^\mu W_{\mu\nu}(P, q) \epsilon^\nu = C \left(-W_1 \epsilon^2 + \epsilon_0^2 W_2 \right), \qquad (60)$$

where $W_{\mu\nu}$ is the same hadronic tensor as introduced above and C is a function containing flux and other factors.

- Introduce *longitudinal* and *transverse cross–section*:

$$\sigma_{\mathrm{T}}(\gamma^* p) \equiv \frac{1}{2} \left(\sigma_{\mathrm{T}}^{(1)} + \sigma_{\mathrm{T}}^{(2)} \right) = \sigma_{\mathrm{T}} = C W_1, \qquad (61)$$

$$\sigma_{\mathrm{L}}(\gamma^* p) = C \left(-W_1 + \frac{q_3^2}{Q^2} W_2 \right) = C \left(-W_1 + \left(1 + \frac{Q^2}{4 M_p^2 x^2} \right) W_2 \right), \; (62)$$

$$\sigma(\gamma^* p) \equiv (\sigma_{\mathrm{T}} + \sigma_{\mathrm{L}}) = C \left(1 + \frac{Q^2}{4 M_p^2 x^2} \right) W_2, \qquad (63)$$

Cross–sections of virtual photons

- So we have
$$CW_1 = \sigma_T \Rightarrow 2xF_1 = \frac{2x}{C}\sigma_T \equiv F_T \tag{64}$$

$$CW_2 = (\sigma_T + \sigma_L)\frac{4M_p^2 x^2}{Q^2 + 4M_p^2 x^2} \Rightarrow F_2 = \frac{2x}{C}\left[\frac{Q^2}{Q^2 + M_p^2 x^2}\right](\sigma_T + \sigma_L) \doteq F_T + F_L, \tag{65}$$

- Defining the ratio:
$$R(x, Q^2) \equiv \frac{\sigma_L(x, Q^2)}{\sigma_T(x, Q^2)} \tag{66}$$

and since
$$\frac{W_2}{W_1} = \left(1 + \frac{\sigma_L}{\sigma_T}\right)\frac{Q^2}{Q^2 + \nu^2} = (1 + R)\frac{Q^2}{Q^2 + \nu^2} \tag{67}$$

we get
$$\frac{2xF_1}{F_2} = \frac{1 + 4M_p^2 x^2/Q^2}{1 + R}. \tag{68}$$

- Introduce so called *longitudinal structure function*
$$F_L(x, Q^2) \equiv F_2(x, Q^2)\left(1 + \frac{4M_p^2 x^2}{Q^2}\right) - 2xF_1(x, Q^2), \tag{69}$$

in terms of which
$$R(x, Q^2) = \frac{F_L(x, Q^2)}{2xF_1(x, Q^2)}. \tag{70}$$

Cross–sections of virtual photons

- Inverting the relations (64)-(65) we get $\sigma_\text{T}, \sigma_\text{L}$ in terms of F_1, F_2:

$$
\begin{aligned}
\sigma_\text{T}(x, Q^2) &= C F_1(x, Q^2), \\
\sigma_\text{L}(x, Q^2) &= \frac{C}{2x}\left[F_2(x, Q^2)\left(1 + \frac{4M_p^2 x^2}{Q^2}\right) - 2x F_1(x, Q^2)\right] = C\frac{F_\text{L}(x, Q^2)}{2x}.
\end{aligned}
\tag{71}
$$

- Similarly inverting (68) we get F_1 in terms of F_2 and R

$$
2x F_1(x, Q^2) = F_2(x, Q^2)\left[\frac{1 + 4M_p^2 x^2/Q^2}{1 + R(x, Q^2)}\right]
\tag{72}
$$

and consequently the brackets of (45) can be written in terms of F_2 and R as follows

$$
F_2(x, Q^2)\left[1 - y + \frac{y^2}{2}\left(\frac{1 + 4M_p^2 x^2/Q^2}{1 + R(x, Q^2)}\right) - \frac{M_p^2 x^2 y^2}{Q^2}\right].
\tag{73}
$$

Cross–sections of virtual photons

- Simultaneous measurement of F_1, F_2 as functions of x, Q^2 is in fact impossible in a single experiment at one primary energy. (73)$\Rightarrow$ separating $F_1(x, Q^2)$ from $F_2(x, Q^2)$ at fixed x, Q^2 is possible only if y can be varied. Since $Q^2 = Sxy$, this requires that the measurement is performed at least at 2 primary energies. Moreover, for this separation the double differential cross–section is usually written as:

$$\frac{d\sigma}{dx dQ^2} = \Gamma \left(\sigma_{\mathrm{T}}(x, Q^2) + \varepsilon(y)\sigma_{\mathrm{L}}(x, Q^2) \right),$$

$$\varepsilon(y) \equiv \frac{2(1-y)}{1 + (1-y)^2}, \ \Gamma \equiv \frac{4\pi\alpha^2}{CQ^4} \left(1 + (1-y)^2 \right). \tag{74}$$

- Note that the function $\varepsilon(y)$ can be interpreted as the ratio of flux factors of longitudinal and transverse virtual photons.

- In terms of $F_2(x, Q^2)$:

$$\sigma(\gamma^* p; W, Q^2) = \frac{CF_2(x, Q^2)}{2x} \frac{Q^2 + 4M_p^2 x^2}{Q^2} =$$

$$\frac{CF_2(W, Q^2)}{2x} \left[\frac{(W^2 - M_p^2) + Q^2 (Q^2 + 2W^2 + 2M_p^2)}{(W^2 - M_p^2) + Q^2 (Q^2 + 2W^2 - 2M_p^2)} \right]. \tag{75}$$

Cross–sections of virtual photons

- For real photons with polarization vector ϵ eq. (21) leads to:

$$\sigma(\gamma p; W\epsilon) = \frac{4\pi^2\alpha}{E_\gamma M_p}\epsilon^\mu\left(-W_1(W,0)g_{\mu\nu} + \frac{P_\mu P_\nu}{M^2}W_2(W,0)\right)\epsilon^\nu, \quad (76)$$

for real photon $C = 4\pi^2\alpha/E_\gamma M_p$.

- Recalling that $E_{\gamma^*} = (W^2 - M^2 + Q^2)/(2M)$ the direct generalization for γ^* would be:

$$C = \frac{8\pi^2\alpha}{W^2 - M_p^2 + Q^2}. \quad (77)$$

- However, for virtual photons the standard definition of C is (77), but *without* Q^2 in its denominator, i.e.

$$C = \frac{8\pi^2\alpha}{W^2 - M_p^2} = \frac{8\pi^2\alpha x}{Q^2(1-x)} \quad (78)$$

so that F_2 and $\sigma(\gamma^* p)$ are then related as follows

$$F_2(x,Q^2) = \sigma(\gamma^* p; W, Q^2)\left[\frac{Q^2}{Q^2 + 4M_p^2 x^2}\right]\frac{Q^2(1-x)}{4\pi^2\alpha}, \quad (79)$$

$$\sigma(\gamma^* p; W, Q^2) = \frac{F_2(x,Q^2)}{Q^2}\left[\frac{Q^2 + 4M^2 x^2}{Q^2}\right]\frac{4\pi^2\alpha}{1-x}. \quad (80)$$

- Keeping Q^2 in denominator of (77) would mean replacing $(1 - x)$ in (79) by unity. Note that as the virtual photon goes on shell, $Q^2 \to 0$, with W kept fixed, $x \to 0$ and the square bracket in (79)-(80) approaches unity

$$\lim_{Q^2 \to 0} \frac{Q^2 + 4M_p^2 x^2}{Q^2} = \lim_{Q^2 \to 0} \frac{(W^2 - M_p^2) + Q^2 (Q^2 + 2W^2 + 2M_p^2)}{(W^2 - M_p^2) + Q^2 (Q^2 + 2W^2 - 2M_p^2)} = 1.$$
(81)

- Consequently $F_2(W, Q^2)$ must behave as $\mathcal{O}(Q^2)$ at small Q^2!

Electrons as tools for investigating nuclear structure

- Rutherford used α-particles for his studies, but already in 1914 Franck and Hertz were first to use the electrons for this purpose.

- Electrons – soon recognized as the best probes of hadrons because $\Leftarrow$ electromagnetic interactions are well-understood.

- Since commissioning of Mark III Linac at Stanford University (Ca.) in 1953 e^- were systematically used by a group led by Robert Hofstadter to investigate structure of nuclei and later also of nucleons.

- The results confirmed what was expected – nuclei have a *finite* size, but also showed that their boundary is not sharp.

- For electron energies (125 and 150 MeV) used in these experiments the momentum transfer $Q = \sqrt{Q^2}$ was restricted to rather small values $Q \leq 0.1$ GeV, corresponding to distances of about 2 fm. Recall in this context that in 1911 Marsden and Geiger managed to restrict the size of gold nuclei to less than about 30 fm.

Electrons as tools for investigating nuclear structure
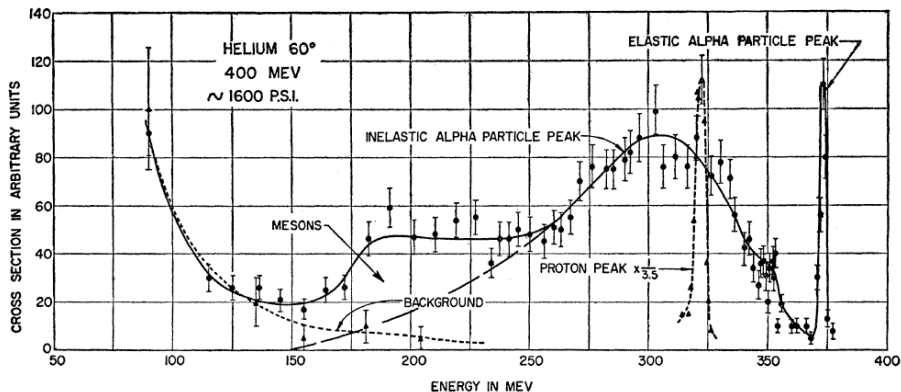
Figure 2: Elastic and inelastic $e^- + {}^4$He scattering. Incident electrons had energy 400MeV, secondary electrons were detected at $\vartheta = 60°$. MESONS refer to π^- produced in the target and emerging with the same momentum as the corresponding scattered electrons. The free proton peak is shown for comparison. From R. Hofstadter, Rev.Mod.Phys.28(1956)214.
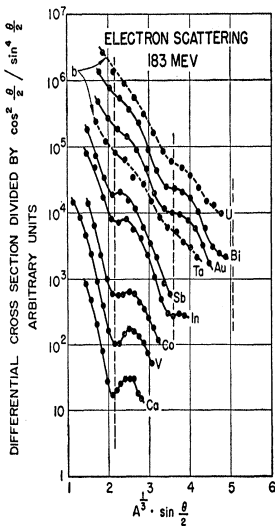
Fig. 41. Experimental results of Hahn *et al.*[33] which show that a radial parameter of the various charge distributions follows an $A^{\frac{1}{3}}$ law. The diffraction features are clearly evident and are emphasized at lower atomic numbers.
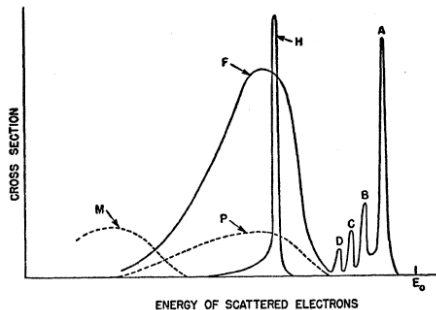
Fig. 53. This figure attempts a summary of the various possible phenomena observed in electron scattering for high momentum transfers. A represents an elastic peak and B, C, D refer to inelastic scattering from nuclear levels. H is the free proton peak observed in hydrogen. P is the incoherent scattering peak of an individual proton (or neutron) in the nucleus. It is broadened with respect to the free proton peak H by motion within the nucleus. F is the simple sum of all such peaks for all the A nucleons in the nucleus. M represents electrons scattered after producing pions. Note that all electrons lie on the low-energy side of E_0 (the incident energy) because of nuclear recoil effects. The figure is not to scale either vertically or horizontally.

From R. Hofstadter, Rev.Mod.Phys.28(1956)214.

Electrons as tools for investigating nuclear structure

- 1955 Hofstadter and his group started to study structure of individual nucleons. Using the detector shown in Fig. 36 and beams of electrons with energies up to 200 MeV, they performed a series of experiments the results of which earned Hofstadter the Nobel prize for physics in 1961.
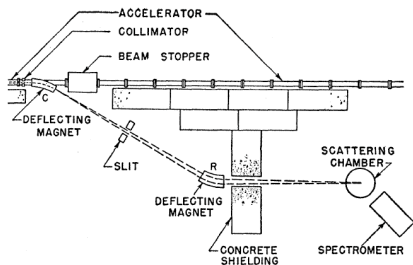

FIG. 14. The general layout of the equipment at the halfway point and the accelerator. Experiments, limited by the spectrometer to 190 Mev, are carried out in this area.
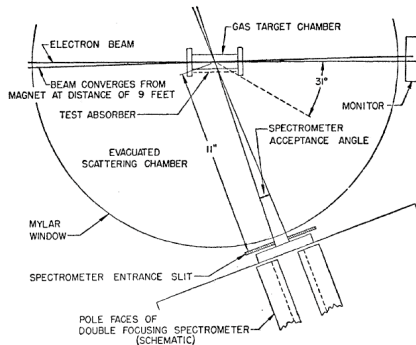
FIG. 17. Schematic diagram of scattering geometry employed with the gas target chamber.

Figure 3: From R. Hofstadter, Rev.Mod.Phys.28(1956)214.

Electrons as tools for investigating nuclear structure

- Hofstadter *et al.* have shown that proton does not behave as a pointlike source of the Coulomb field, but rather as a particle with *finite* $r \approx 1$fm.

- $e^- + p$ differential cross section differs from that of pointlike proton ("Dirac curve") as well as from that which includes anomalous part of μ_p as given by the formula (40) with $F_1 = 1$, $F_2 = 1.793$ ("anomalous curve") (see left part of Fig. 4). The fact that the latter curve is above the data had been interpreted as evidence that the proton "is not a point".

- Fitting the experimental distribution in the left plot of Fig. 4 to the Mott cross section multiplied by the form factor (assumed the same for charge and magnetic moment) lead to the determination of root–mean–square radius of the proton $r_{ch} = r_{mag} = 0.7 \pm 0.24$fm.

- In 1955 E_e was increased to 550 MeV extending measurements into the region $Q^2 \leq 0.5$ GeV^2. The main result – Q^2-dependence of proton formfactors – is shown on the right plot in Fig. 4.

- Investigations were completed in early sixties using 1000 MeV electron beam from the upgraded Mark III Linac which showed that within the accuracy of the measurement the charge and magnetic formfactors coincide, as assumed in the earlier work.

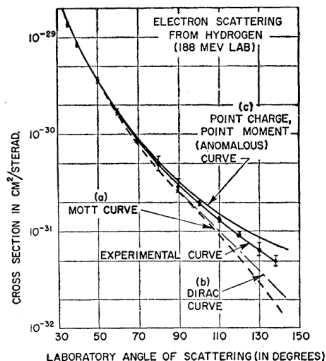# Electrons as tools for investigating nuclear structure

FIG. 24. Electron scattering from the proton at an incident energy of 188 Mev. The experimental points lie below the point-charge point-moment curve of Rosenbluth, indicating finite size effects.
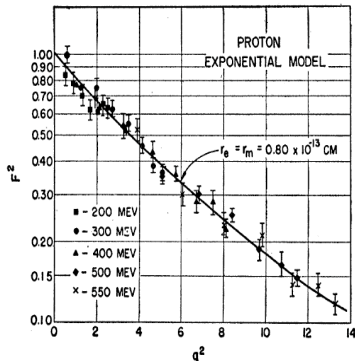

FIG. 27. The square of the form factor plotted against q^2. q^2 is given in units of 10^{-26} cm². The solid line is calculated for the exponential model with rms radii=0.80×10^{-13} cm.

Figure 4: Left: Comparison of data with theoretical calculations described in the text. The best fit corresponds to exponential charge distribution with r.m.s. radius equal to 0.74 fm. Right: Q^2 dependence of proton formfactors plotted in units of inverse square fm, which means that the point 12.5 fm^{-2} corresponds to $Q^2 = 0.5$ GeV^2.

From R. Hofstadter, Rev.Mod.Phys.28(1956)214.

What $e^- + p$ DIS tells us about the structure of nucleons?

- The success of 1 GeV Linac at Stanford led to the decision to built a new electron linear accelerator with energies up to 20 GeV, using the infrastructure available at the newly created Stanford Linear Accelerator Center (SLAC).

- Aim was to extend elastic scattering experiments and also to investigate quasi-elastic scattering, i.e. the electroproduction of resonances, like Δ, etc.

- Just for completeness the group also wanted to look at the inelastic continuum, which was inaccessible in previous Hofstadter's experiments. However, the planning of the machine was not influenced by any considerations that possible point-like substructure of the nucleon might be observed in electron scattering!

- The two miles long machine was commissioned in late 1966 and in 1967 the group of experimentalists from SLAC and MIT started a series of experiments aiming primarily at the investigation of elastic electron proton scattering in much wider range of momentum transfer Q^2, but making possible also the first serious study of deep inelastic electron-proton scattering.
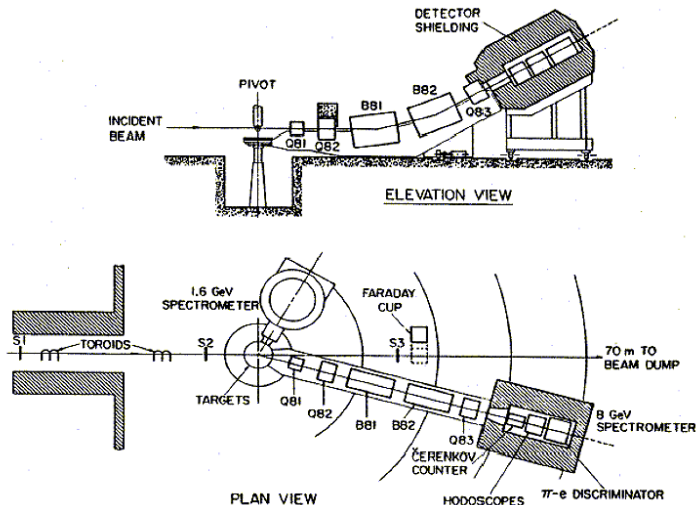
Figure 5: Schematic layout of the spectrometer used in experiments with deep inelastic scattering of electrons on protons at SLAC.

What $e^- + p$ DIS tells us about the structure of nucleons?

- First results obtained in early 1968 concerned elastic and inelastic formfactor $G_M \equiv F_1 + \kappa F_2$. Fit to the elastic formfactor by the dipole formula gave $(1/(1 + Q^2/0.71))^2$.

- Data on inelastic formfactor at fixed W and also their possible scaling behavior are shown in Fig.6. SLAC experimentalist concluded "...*data might give evidence on the behavior of point-like charged structures in the nucleon.*"

- This point of view was not shared by the theorists at that time. There were few clear ideas about Q^2-dependence of inelastic formfactors and in particular on behavior of structure functions $F_1(x, Q^2)$ and $F_2(x, Q^2)$ as functions of Q^2 for W^2 outside the resonance region, i.e. for $W^2 = Q^2(1 - x)/x \gtrsim 2$ GeV^2, in the limit $Q^2 \to \infty$. Will they vanish as rapidly as the elastic formfactors or could they eventually approach nonzero functions of x?

- Shortly before the first data from SLAC appeared Bjorken had suggested the latter possibility – now called *Bjorken scaling*, but his derivation was based on several questionable assumptions and few other theorists, perhaps including Bjorken himself, took it seriously.

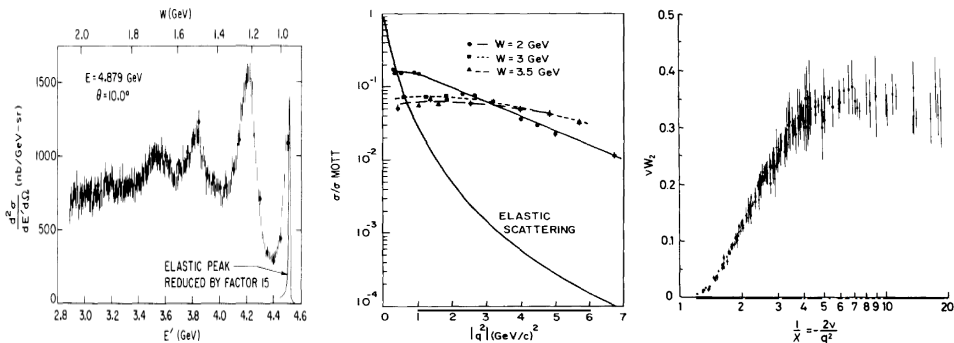# First SLAC results on $e^- + p$ DIS

Figure 6: *Left:* Doubly diff. cross-section (in nb/GeV. sr) for scattering of incident 4.9 GeV electrons on hydrogen at $10°$ versus detected e^- energy, E (in GeV). Scale at the top (W) is invariant mass of the undetected hadronic system.
Middle: Ratio σ/σ_{MOTT} (which is directly proportional to the structure functions) versus q^2 for various values of W. This is basically another representation of the kinds of data shown on the left panel. For comparison the elastic data is shown on the same plot.
Right: Scaling form of the data shown on left and middle panels. Dimensionless combination νW_2 is plotted versus the dimensionless variable $\omega = 1/x = 2\nu/q^2$ for many values of q^2. The various points seem to lie on a universal curve.

What $e^- + p$ DIS tells us about the structure of nucleons?

- Although the quark model had been formulated three years earlier and had some success in explaining the static properties of nucleons, almost nobody thought it might be relevant for the dynamics of high energy e+p scattering.

- To illustrate the prevalent mood of that time, let's quote Gell-Mann's introductory talk at conference held in Berkeley in Summer 1967, just at the time the first measurements at SLAC were under way:

We consider three hypothetical and probably fictitious spin 1/2 quarks, ...
It is possible that real quarks exist, but if so they have high threshold for copious production, many GeV; if this threshold comes from their rest mass, they must be very heavy and it is hard to see how deeply bound states of such heavy real quarks could look like $q\bar{q}$, say, rather than a terrible mixture of $q\bar{q}$, $qq\bar{q}\bar{q}$, and so on. Even if there are light real quarks and the threshold comes from very high barrier, the idea that mesons and baryons are made primarily of quarks is difficult to believe ...
The probability that a meson consists of a real quark pair rather than two mesons or a baryon and antibaryon must be quite small. Thus it seems to me that whether or not real quarks exist, the q or $\bar{q}$ we have been talking about are mathematical entities that arise when we construct representations of current algebra, which we shall discuss later on...

Bjorken and Callan–Gross sum rules for DIS

- The only theoretical framework for the analysis of inelastic electron-proton scattering at that time was based on the analytic properties of the scattering matrix. Within this framework, and using rather heavy artillery of the so called "current algebra", it was possible to derive several relations involving measurable quantities.

- For instance, Bjorken derived the following restriction on the integrals over the structure functions $F_2^p(x, Q^2)$ and $F_2^n(x, Q^2)$:

$$\frac{1}{M} \int \mathrm{d}\nu \left[W_2^p(\nu, Q^2) + W_2^n(\nu, Q^2) \right] = \int \frac{\mathrm{d}x}{x} \left[F_2^p(x, Q^2) + F_2^n(x, Q^2) \right] \geq \frac{1}{2}. \tag{82}$$

- Callan and Gross derived the sum rule for similar combination:

$$\frac{Q^2}{2M^2} \int \frac{\mathrm{d}\nu}{\nu} \left[W_2^p(\nu, Q^2) + W_2^n(\nu, Q^2) \right] = \int \mathrm{d}x \left[F_2^p(x, Q^2) + F_2^n(x, Q^2) \right] \leq \frac{1}{2}, \tag{83}$$

which should hold in the limit $Q^2 \to \infty$.

- *In both cases no assumption concerning the structure of the nucleon was made.*

Yet another DIS sum rule: Gottfried sum rule

- Assuming the constituent quark model, Gottfried derived the sum rule for $W_2^p(x, Q^2)$ itself

$$\frac{1}{M} \int d\nu\, W_2^p(\nu, Q^2) = \int \frac{dx}{x} F_2^p(x, Q^2) = 1 - \frac{G_E^2(Q^2) + (Q^2/4M^2) G_M^2(Q^2)}{1 + Q^2/4M^2}$$

$$\simeq 1 - \frac{1 + 2.2Q^2}{(1 + 0.29Q^2)(1 + 1.4Q^2)^4} \xrightarrow[Q^2 \to \infty]{} 1, \tag{84}$$

  where the proton elastic formfactors G_M and G_E were fitted by the common form $(1/(1 + Q^2/0.71))^2$.

- James Bjorken, September 1967: *But the indication is that there does not yet seem to be any large cross sections which this model of point-like constituents suggests. Additional data is necessary and very welcome in order to completely destroy the picture of elementary constituents.*

- Kurt Gottfried's comment following Bjorken's talk: *I think Professor Bjorken and I constructed sum rules in hope of destroying the quark model.*

What $e^- + p$ DIS tells us about the structure of nucleons?

- Although Bjorken's suggestion proved to be wrong if taken literally, it prepared the ground for the concept of *approximate scaling*, which was observed at SLAC and which became the starting point for Feynman's parton model to be discussed below. Today we know that within Quantum Chromodynamics the structure functions $F_i(x, Q^2)$ vanish for any fixed $x > 0$ when $Q^2 \to \infty$. However, and this is the crucial point, they do so *very slowly*, much more slowly than the elastic formfactors of nucleons!

- In fact, had the theorists in late sixties taken the idea that nucleons are in some sense composite objects, the slow Q^2-dependence of structure functions describing the deep inelastic electron-proton scattering could be expected on quite general grounds. Even for very large Q^2 it is in principle possible that the momentum transferred to the nucleon will dissipate among its constituents in such a way that the nucleon will not break up but will recoil as whole but this process will be very rare. Hence the Q^2-dependence of G_M and G_E. $G_E(Q^2) \simeq G_M(Q^2) \propto 1/Q^4$ for large Q^2 t (implying $1/Q^8$ dependence of elastic cross sections!).

- In most cases the nucleon experiencing hard collision with an electron will break up leading to final states with typically many particles. The probability
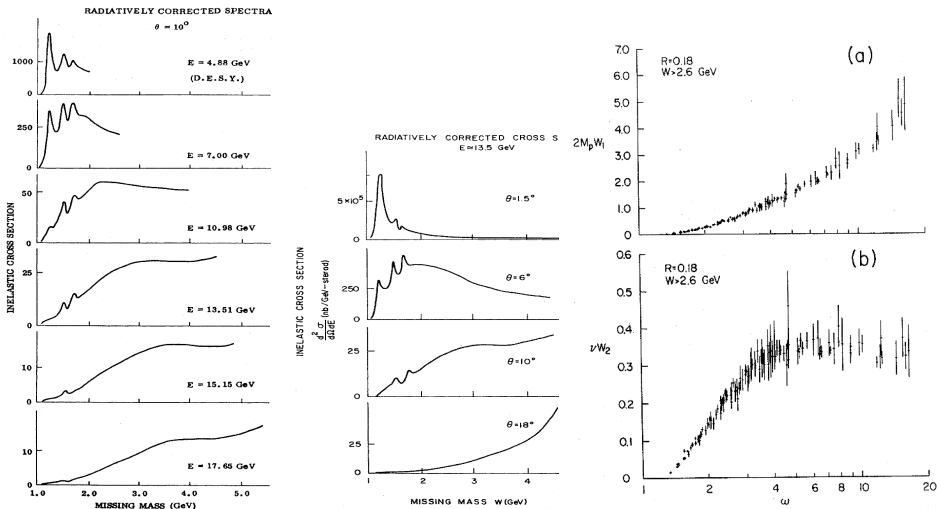
Figure 7: *Left:* Visual fits to $e^- + p$ scattering at $10°$ for E=4.88–17.65 GeV. Elastic peaks have been substracted. *Middle:* Visual fits to $e^- + p$ scattering at $1.5°$–$18°$ for E=13.5 GeV. *Right:* Scaling $F_1 = 2MW_1(\omega)$ vs ω and $F_2 = \nu W_2(\omega)$ vs ω.

From Henry W. Kendall, Rev.Mod.Phys.63(1991)597

What $e^- + p$ DIS tells us about the structure of nucleons?

- Despite this low expectations, the data on DIS, some of which are reproduced in Fig. 7, turned out to be both surprising and of far-reaching consequences. In recognition of their importance for the development of parton model and eventually the formulation of QCD, R. Taylor, H. Kendall and J. Friedman were awarded the 1990 Nobel Prize for Physics.

- The main features of these results are the following (the notation used in Fig. 7 is related to that used in this text as follows:
$\nu W_2 = F_2, \omega = 1/x, W^2 = -Q^2 + M_p^2 + 2M\nu = Q^2(1-x)/x + M_p^2$):

  1. Varying energy of the electron beam allowed to determine, for a fixed pair x, Q^2, separately the two structure functions $F_1^p(x, Q^2)$ and $F_2^p(x, Q^2)$. Measured value of the ratio (70) $R = 0.18$ was then used in the following considerations.

  2. In the resonance region, i.e. for $W^2 \simeq 1 - 4$ GeV, the $F_2(W^2, Q^2)$ rapidly falls off with increasing Q^2, similarly as the elastic formfactor $F_2(Q^2)$. Three resonances are visible in the upper left plot of Fig. 7, first corresponding to $\Delta(1236)$. Their positions as functions of ν move with increasing Q^2 to the right reflecting the fact that $\nu = (W^2 + Q^2)/2M_p$.

What $e^- + p$ DIS tells us about the structure of nucleons?

3. On the other hand, in the continuum region, i.e. roughly for $W \gtrsim 2$ GeV, $F_2^p(x, Q^2)$ varies with Q^2 only very slowly. This is shown in the right part of Figs. 6 and 7.

4. In this region the data are moreover consistent with the Bjorken scaling hypothesis. This is suggested by the right plot of Fig. 7 which shows the approximate constancy of $F_2(\omega, W^2)$ considered as a function of $W^2 = Q^2(\omega - 1) + M_p^2$ for fixed $\omega = 1/x$, and in the lower left plot as the approximate Q^2-independence of $F_2(x = 1/\omega, Q^2)$ considered as a function of $\omega = 1/x$.

5. Integrating over the accessible kinematical region of both x and Q^2 gave the following values for two important sum rules mentioned above.

$$I_1^{\mathrm{p}} = \int_{0.05}^1 \frac{\mathrm{d}x}{x} F_2^p(x, Q^2) = 0.78 \pm 0.04, \quad I_2^{\mathrm{p}} = \int_{0.05}^1 \mathrm{d}x F_2^p(x, Q^2) = 0.172 \pm 0.009.$$

(85)

Emergence of the parton model

- Feynman, during several visits to SLAC in Autumn 1968, using the intuitive language of parton distribution functions (PDF), developed the basic ideas of the *parton model*.

- PDF remain the basic theoretical concept also in QCD.

- Basic idea of parton model is to represent deeply inelastic ($Q^2 \gg M_p^2$) electron-nucleon scattering as *quasi-free scattering from point-like constituents* within the proton when viewed from a frame in which $P \to \infty$.

- At high energies $e + p$ c.m.s. is a good approximation of such a *infinite momentum frame* (IMF).

- Despite the fact that any frame is in principle as good as IMF and we use manifestly relativistic invariant variables like x, y or Q^2 this choice of a preferred reference frame (or, better, family of frames) is at the heart of the parton model. For instance, parton model cannot be easily formulated in proton rest frame.

Parton model

- In IMF p_T of proton constituents induced by the internal "Fermi motion", characterized by $p_T \lesssim M_p$, as well as the masses of nucleons and partons can be neglected with respect to the longitudinal
  $\Rightarrow$ the parton four-momentum is $p = \eta P$.

- In $e + p$ DIS these transverse components can be safely neglected also in the evaluation of the corresponding cross section, which can be written as an **incoherent sum** of cross sections from elastic scattering on individual charged partons.

- Momentum conservation at the lower vertex in Fig. 1c,

$$(p')^2 = (p + q)^2 = p^2 + q^2 + 2pq \Rightarrow 2pq = -q^2 = Q^2 \qquad (86)$$

implies that the variable x in (5) coincides within the parton model with fraction η introduced above.

Parton model

- The above quasi-free electrons-parton scattering model is sufficient for calculation $d\sigma/dxdQ^2$ of inclusive electron-proton scattering, which depend on the kinematical variables describing the scattered electron only.

- Comparing (37) for the scattering on pointlike fermion with spin $1/2$ with the general form (45) for the scattering on the proton we see that the last, mass terms, coincide provided we identify $M = xM_p$, i.e. the rest mass of interacting quarks should depend on its momentum! $\Rightarrow$ parton model is noncontradictory only for the *massless* protons and partons, i.e. in the IMF. In practice parton model is relevant any when $Q^2 \gg m_p, m_q$.

Parton model

- Feynman had also added the basic mechanism of **hadronization** i.e. the conversion of final state partons into observable hadrons which occurs *much later* than the scattering of electrons from partons and *does not* therefore influence it. The overall picture of the collision is sketched in Fig. 8.
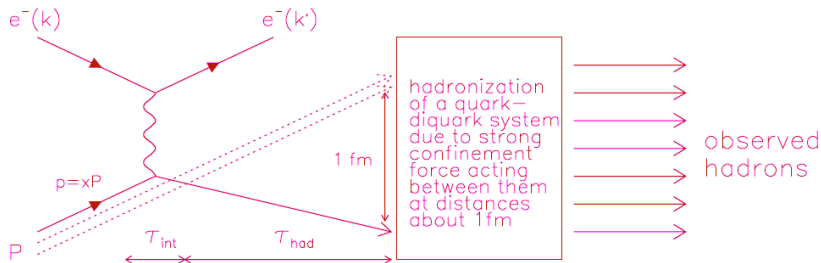

Figure 8: DIS on a real proton in the parton model. The incoming electron scatters on a single parton, while the remaining diquark flies unperturbed on, until the forces of confinement, acting between them at distances larger than about 1 fm, cause their conversion into observable hadrons. For this picture to be consistent the time separation τ_{had} between these two stages must be significantly larger than the characteristic time τ_{int} of the electron–parton scattering.

Parton model

- Consider now $\mathrm{d}\sigma/\mathrm{d}x\mathrm{d}Q^2$ as given in (46) at large energies. i.e.

$$\frac{\mathrm{d}\sigma}{\mathrm{d}x\mathrm{d}Q^2} \underset{kp\to\infty}{\longrightarrow} \frac{4\pi\alpha^2}{Q^4}\frac{F_2(x,Q^2)}{x}, \qquad (87)$$

where only one structure function appears. In this limit the differential cross section of elastic scattering of electrons from a pointlike fermion or boson of electric charge e_p, given in (38) for unit electric charge, equals

$$\frac{\mathrm{d}\sigma}{\mathrm{d}Q^2} = \frac{4\pi\alpha^2 e_p^2}{Q^4}\left[1 - y + \varepsilon\frac{y^2}{2} - \frac{M_p y}{2kp}\right] \underset{kp\to\infty}{\longrightarrow} \frac{4\pi\alpha^2 e_p^2}{Q^4} \qquad (88)$$

and is thus the same for both types of partons.

- Feynman wrote: $\qquad \dfrac{F_2(x)}{x} = \displaystyle\sum_i e_i^2 d_i(x) \Rightarrow F_2(x) = x\sum_i e_i^2 d_i(x) \qquad (89)$

where functions $d_i(x)$ describe the probability to find inside the proton parton species i with fraction x of proton momentum and electric charge e_i.

- N.B. Approximate scaling, i.e. independence of the measured $F_2(x,Q^2)$ of Q^2 is clearly indispensable for this expression to make sense.

Parton distribution function: simple model

- Simple parton distribution function (PDF) model:
  proton is superposition of states with different, but fixed, number of partons. The simplest one – in the N-parton configuration, which appears in the proton with the probability $P(N)$, all partons carry the same momentum fraction $x_N = 1/N$ and thus

$$F_2(x) = \sum_N P(N) \frac{\delta(x - 1/N)}{N} \langle \sum_{i=1}^{N} e_i^2 \rangle$$

$$\Rightarrow \int_0^1 \mathrm{d}x F_2(x) = \sum_N P(N) \frac{\langle \sum_{i=1}^{N} e_i^2 \rangle}{N}, \qquad (90)$$

where $\langle \sum_{i=1}^{N} e_i^2 \rangle / N$ is the mean square electric charge in the N-parton configuration. In this model the integral I_2^{p} defined in (85) can thus the interpreted as mean square charge per parton in the proton. In fact this interpretation holds in the whole class of models of distribution functions $d_i(x)$ in which the N-parton distribution function $f(x_1, x_2, ..., x_N)$ is a symmetric function of its arguments.

Parton spin

- For $\sqrt{S} \to \infty$, only $F_2(x, Q^2)$ structure function appears. At finite energies also $F_1(x, Q^2)$ contributes $\Rightarrow$ one may extract both of them from (74), which requires measurements for fixed x, Q^2 at two energies. This has, indeed, been done at SLAC with the results $R = 0.18$, which implies that to a good approximation the measured structure functions satisfy the so called *Callan-Gross relation* $F_2(x) = 2xF_1(x)$.

- This in turn means that *charged partons are fermions with spin 1/2*! Note that for scalar partons (37) implies $F_1(x) = 0$, which is clearly ruled out by data. The same holds for vector, i.e. spin 1, gluons, which provides one of the experimental facts for ruling out the Hahn-Nambu model of integral charge colored quarks.

- The spin $1/2$ nature of charged partons, suggested by data, immediately raised the question of their relation to the **constituent quarks** of the additive quark model. Although these two concepts are *not* identical it has become practice to call the original parton model of Feynman in which the basic charges constituents of nucleons are identified as far as their quantum numbers are concerned with quarks, the *Quark Parton Model* and denoted QPM.

Parton spin

- N.B. The charged, spin $1/2$ partons, introduced by Feynman, are usually called *current quarks* (of definite flavor) to emphasize this difference. Compared to the constituent quarks they are light (about 10 MeV for u, d quarks compared to roughly 300 MeV for the constituent ones) and there is no fixed number of them inside the proton.

- Contradiction: QPM assumes that e^- scatter on *free* quarks, despite the fact that no quarks have so far been observed in the nature and thus one would expect them to be *tightly* bound inside the proton (and other hadrons). This has originally been the source of suspicion of many physicists. The reason why the QPM nevertheless works was explained by the asymptotic freedom of QCD later on.

- Experimentally F_1, F_2 were found in fact not exactly Q^2-independent, as assumed in the QPM, but depend, as indicated already by the original SLAC measurements, also weakly on Q^2. This weak Q^2 dependence will be ignored in this chapter. We shall return to it later when dealing with the description of these *scaling violations*.
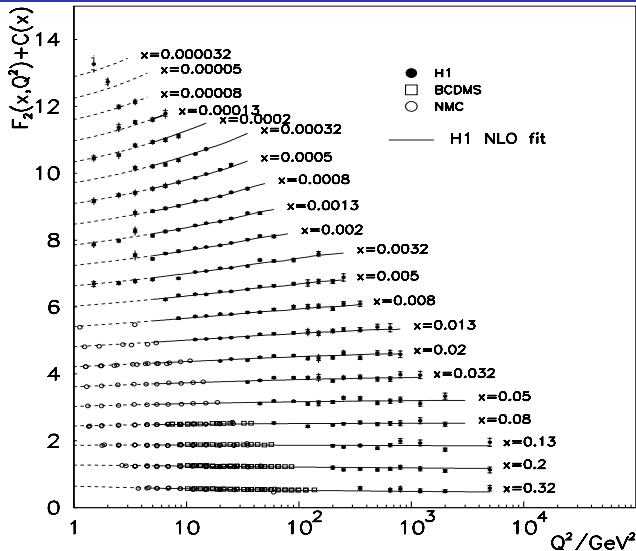
Figure 9: The Q^2 dependence of the proton structure function $F_2^{ep}(x, Q^2)$ for several fixed values of x. Old SLAC data are complemented by the recent results from the H1 Collaboration at DESY. From S. Aid *et al.*, Nucl.Phys.B470(1996)3.

$F_2(x, Q^2)$: SLAC results

- Measured value of $I_2^{\mathrm{p}} = 0.17 \pm 0.009$, representing in the parton model the mean square charge per parton in the proton, was about half the value $1/3 = (4/9 + 4/9 + 1/9)/3$ expected in the simplest form of the parton model.

- Bjorken and Paschos: *"the observed cross section is uncomfortably small"* even if the three quarks were supplemented by the sea of quark-antiquark pairs.

$\Rightarrow$ The data clearly indicated that *there must be also electrically neutral partons in the proton* but it took another year, until the invention of QCD in 1973, to realize it.

Parton distribution functions and their basic properties

- From now on the distribution functions $d_i(x)$ of current quarks inside the proton will be denoted as $q(x)$, $q = u, d, s, c$ and as $\overline{q}(x)$ for the corresponding antiquarks. Pdf of bottom and top quarks does not make much sense $\Leftarrow$ they are too heavy for that purpose.

- N.B. Isospin symmetry $\Rightarrow$ the same pdf can be used for also neutron. i.e. u-quark in the proton is the same as d-quark in the neutron and vice versa.

- It took a lot of work to extract from vast amount of experimental data on F_1, F_2 pdf of individual current quarks $\Rightarrow F_1, F_2$ are always combinations of the latter, for instance:

$$F_2^{\text{ep}}(x) = x \left(\frac{4}{9}[u(x) + \overline{u}(x) + c(x) + \overline{c}(x)] + \frac{1}{9}[d(x) + \overline{d}(x) + s(x) + \overline{s}(x)] \right),$$
$$\tag{91}$$

$$F_2^{\text{en}}(x) = x \left(\frac{4}{9}[d(x) + \overline{d}(x) + c(x) + \overline{c}(x)] + \frac{1}{9}[u(x) + \overline{u}(x) + s(x) + \overline{s}(x)] \right).$$
$$\tag{92}$$

- N.B. In going from (91) to (92) we exploited the *isospin* symmetry of quark distribution functions and furthermore assumed that the $s, c, \overline{s}, \overline{c}$ distributions are the same in protons and neutrons.

Parton distribution functions and their basic properties

- A particularly useful combination is the average $F_2^{\mathrm{eN}} \equiv \frac{1}{2}\left(F_2^{\mathrm{ep}} + F_2^{\mathrm{en}}\right) =$

$$= \frac{5}{18} x \underbrace{\left[u(x) + d(x) + \overline{u}(x) + \overline{d}(x) + s(x) + \overline{s}(x) + c(x) + \overline{c}(x)\right]}_{\Sigma(x)} - \frac{1}{6} x k(x),$$

(93)

where $k(x) \equiv (s(x) + \overline{s}(x) - c(x) - \overline{c}(x)) \ll \Sigma(x)$. This combination (93) corresponds to the **isoscalar** target and is measured in experiments using nuclear targets.

- Figs. 10, 11 and 12 display quark and antiquark distribution functions multiplied by x at $Q^2 = 100 \ \mathrm{GeV}^2$ as extracted by three recent *global analyses*, and one older parameterization (denoted HMRSB).

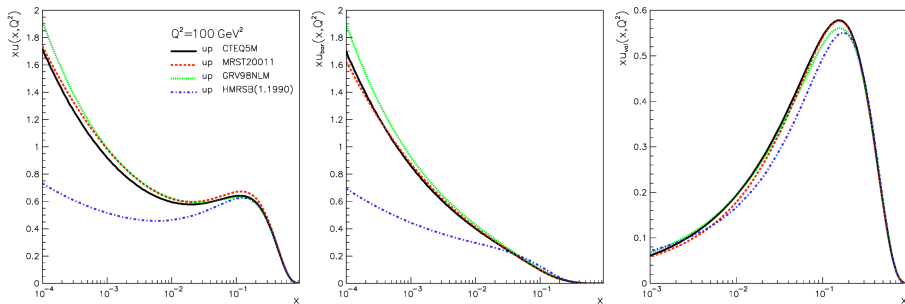# Parton distribution functions and their basic properties

Figure 10: Parton distribution functions of u-quarks (left), $\bar{u}$-quarks (middle) and valence u-quarks (right) in the proton for $Q^2 = 100$ GeV^2 as extracted by four different parameterizations, taken from the CERN PDFLIB library of distribution functions. The first three are the recent ones obtained by CTEQ, MRS and GRV groups, the last one (dash-dotted curves) corresponds to a MRS parametrization more than a decade old.
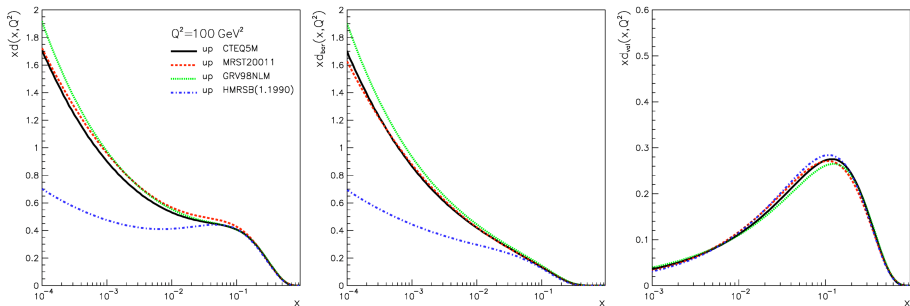
Parton distribution functions and their basic properties

Figure 11: Parton distribution functions of of d-quarks (left), $\overline{d}$-quarks (middle) and valence d-quarks (right) in the proton for $Q^2 = 100$ GeV^2 as extracted by four different parameterizations, taken from the CERN PDFLIB library of distribution functions. The first three are the recent ones obtained by CTEQ, MRS and GRV groups, the last one (dash-dotted curves) corresponds to a MRS parametrization more than a decade old.
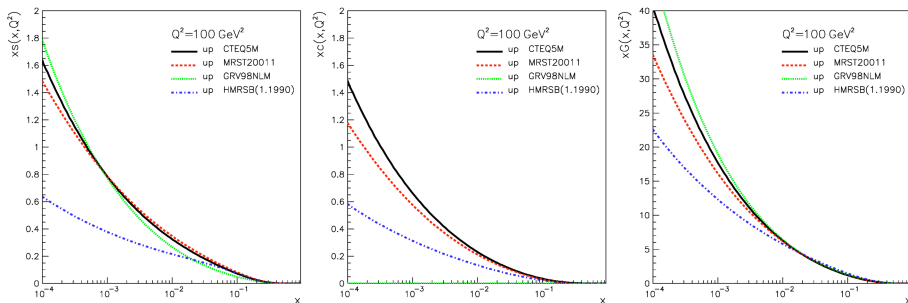
Figure 12: Parton distribution functions of of s-quarks (left), c-quarks (middle) and gluons (right) in the proton for $Q^2 = 100$ GeV^2 as extracted by four different parameterizations, taken from the CERN PDFLIB library of distribution functions. The first three are the recent ones obtained by CTEQ, MRS and GRV groups, the last one (dash-dotted curves) corresponds to a MRS parametrization more than a decade old.

- In global analyses, which will be described in more detail in Section *QCD improved quark-parton model*, one attempts to describe a wide range of physical process with the same set of parton distribution functions.

- The marked improvement in the determination of PDF from experimental data achieved over the last decade has been the consequence of several facts: improvement in the precision and scope of experimental data, progress in perturbative calculations and closer collaboration between experimentalists and theorists in the extraction procedure.

Parton distribution functions and their basic properties

There are two important features of quark distribution functions displayed on Figs. 10, 11 and 12:

1. For $x \to 0$ both $q(x) \sim x^{-1}$ and $\overline{q}(x) \sim x^{-1}$ $\Rightarrow$ integrals

$$\int_0^1 q(x)\mathrm{d}x \quad \text{and} \quad \int_0^1 \overline{q}(x)\mathrm{d}x \quad \text{diverge} \tag{94}$$

$\Rightarrow$ Number of charged partons in the proton is *infinite*. However, this does not presents a serious problem for the QPM.
Consider the so called **valence** distribution functions:

$$q_{val} \equiv q(x) - \overline{q}(x); \quad q = u, d, s, c \tag{95}$$

The data on u_{val} and d_{val} indicate that these functions are *integrable* (see Figs. 10, 11) and the values

$$\int_0^1 u_{val}(x)\mathrm{d}x \doteq 2; \quad \int_0^1 d_{val}(x)\mathrm{d}x \doteq 1 \tag{96}$$

are consistent with the prediction of the additive quark model.

Parton distribution functions and their basic properties

1. (Cont'd)   One can test these relations by evaluating the integral:

$$GS \equiv \int_0^1 \frac{F_2^{\mathrm{ep}}(x) - F_2^{\mathrm{en}}(x)}{x}\mathrm{d}x = \frac{1}{3}\int_0^1 (u_v(x) - d_v(x))\mathrm{d}x - \frac{2}{3}\int_0^1 (\overline{d}(x) - \overline{u}(x))\mathrm{d}x, \tag{97}$$

which should be equal to $1/3$, if $\overline{u}(x) = \overline{d}(x)$ (isospin symmetry). Nevertheless a recent measurement by the NMC Collaboration at CERN yields GS=0.235 ± 0.026, clearly inconsistent with $1/3$. Interpretation of this discrepancy is the *isospin violation* in the sea quark distributions.

2. Fraction of the proton momentum carried by the quark q is

$$\int_0^1 xq(x)\mathrm{d}x; \quad q = u, d, s \tag{98}$$

$\Rightarrow$ fraction of the proton momentum carried by all u, d, s and c quarks and antiquarks together is:

$$\int_0^1 x\Sigma(x)\mathrm{d}x \doteq \frac{18}{5}\int_0^1 F_2^{\mathrm{eN}}(x)\mathrm{d}x, \tag{99}$$

Experimental value is ≈ 0.5 $\Rightarrow \exists$ other, electrically neutral, partons in the proton, carrying the remaining half of its momentum (*gluon*, to be discussed in the section on QCD).

Parton distribution functions and their basic properties

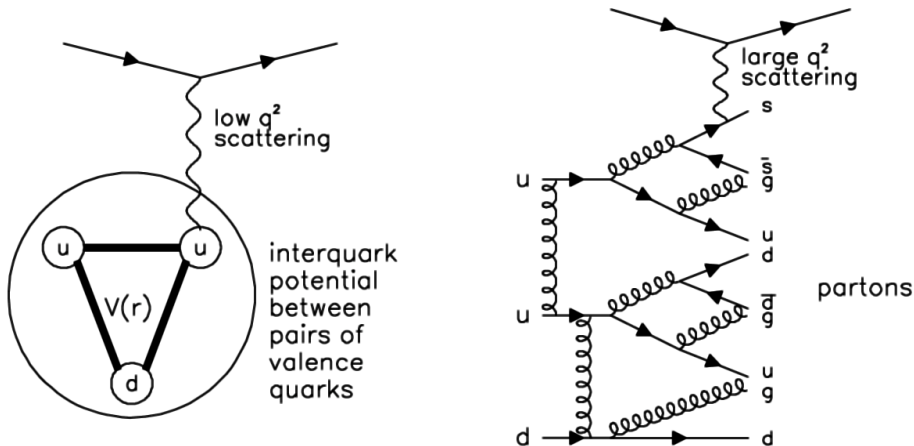- Present understanding of the origin of antiquarks and gluons inside the proton is indicated in Fig. 13.

Figure 13: Field theoretic "explanation" of the generation of partons from valence quarks interacting via the exchange of gluons, carriers of strong force.

Field theoretic generation of partons from valence quarks

- At small resolution (i.e. in the small momentum transfer scattering), proton behaves as a system of three massive **constituent** quarks, bound together by a static potential.

- With higher resolution power, provided by the hard scattering processes, static potential gives rise to gluons which in turn convert to pairs of quarks and antiquarks, which again radiate gluons and so on and so forth. All the created quarks and gluons are **virtual** and thus have to recombine after some time, but if their virtuality[1] is small compared to $\sqrt{Q^2}$, where Q^2 is some measure of the "hardness" of the collision, they will "live" long enough for the probe electron to scatter on them (nearly) as on the real ones.

- This intuitive explanation will be corroborated by more quantitative arguments and calculations in next lecture – *Parton model in other processes*.

---

(1) Measured by the "off–mass shellness" $k^2 - m^2$, where k and m are the momentum and mass of the virtual particle.

Parton model in neutrino interactions

- $u(x)$ and $d(x)$ (in the proton) can be divided into the **valence** parts, defined in (95), and the **sea** parts, which are by definition identical to the antiquark distribution functions:

$$\begin{aligned} \overline{u}(x) &= \overline{u}_{sea}(x) &= u_{sea}(x), \\ \overline{d}(x) &= \overline{d}_{sea}(x) &= d_{sea}(x). \end{aligned} \qquad (100)$$

  s and c-quark pdf of proton have only sea components. Isospin symmetry is usually assumed for the sea distributions. On the other hand, the strange sea in the proton is expected to be suppressed with respect to u_{sea}, due to bigger current mass of the s quark.

- Weak interactions *do distinguish* quarks from antiquarks.

- $\Rightarrow$ With the advent of intense beams of ν_μ and $\overline{\nu}_\mu$ at CERN and Fermilab in the early seventies the $\nu + N$ DIS in the *charged current* (CC)

$$\nu_\mu + N \rightarrow \mu^- + \mathrm{anything} \qquad (101)$$

  as well as *neutral current* (NC) channels

$$\nu_\mu + N \rightarrow \nu_\mu + \mathrm{anything} \qquad (102)$$

  has opened new ways of testing the parton model and contributed decisively to the extraction of distribution functions of individual quark flavors.
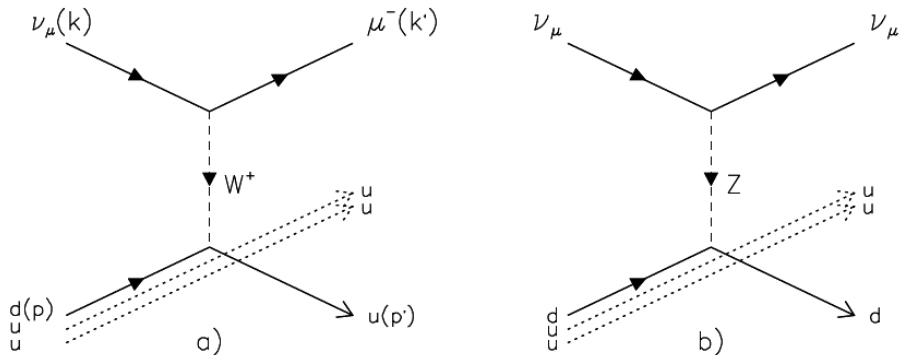
Figure 14: Lowest order Feynman diagrams describing the weak interaction of neutrinos with the exchange of W^+ (a) and Z (b) intermediate vector bosons.

Parton model in neutrino interactions

- In most of the existing applications the exchange of vector bosons $W^{\pm}$ can be replaced by the **effective four–fermion vertex** of the original Fermi theory[1] which takes the form of product

$$\frac{G_F}{\sqrt{2}} J_\mu^{(\ell)} \left(J^{(h)\mu} \right)^+ + \text{h.c.},\tag{103}$$

of the leptonic and quark currents $J_\mu^{(\ell)}$, $J_\mu^{(h)}$

$$J_\mu^{(\ell)} = \sum_{\ell,\ell'} \overline{u}_{l'}\gamma_\mu(1-\gamma_5)u_l + \sum_{\ell,\ell'} \overline{v}_\ell\gamma_\mu(1-\gamma_5)v_{\ell'},\tag{104}$$

$$J_\mu^{(h)} = \sum_{q,q'} \overline{u}_{q'}\gamma_\mu(1-\gamma_5)V_{qq'}u_q + \sum_{q,q'} \overline{v}_q\gamma_\mu(1-\gamma_5)V_{q'q}v_{q'},\tag{105}$$

where the sums run over the pairs of leptons ℓ, ℓ' and quarks q, q' for which $\Delta_\ell \equiv e_\ell - e_{\ell'} = \Delta_q \equiv e_q - e_{q'} = +1$.

(1) This is a good approximation so long as the momentum transfer at the leptonic vertex in Fig. 14 is much smaller than its mass, i.e. $Q^2 \ll M_W^2$.

Parton model in neutrino interactions

- The *unitary* matrix $V_{qq'}$, called *Cabbibo matrix*, describes the **mixing** of quarks (antiquarks) with electric charge $-1/3$ ($1/3$). The unitarity of this matrix implies that for *fully inclusive* quantities, i.e., so long as we *sum* over all final states in (101), $V_{q,\bar{q}}$ can be replaced in (105) by a unit matrix.

- In (104) and (105) Dirac bispinors u, v describe the in– and outgoing states of leptons and quarks (u) and their antiparticles (v), participating in the basic parton level scattering process:

$$\ell(k) + q(p) \rightarrow \ell'(k') + q'(p'). \tag{106}$$

- Consider first the scattering of a *massless* neutrino on the quark with mass M. The spin averaged matrix element squared corresponding to one particular term of (103) is proportional to the contraction of leptonic and quarkonic tensors

$$L_{\mu\nu}^{(1)} L_{(2)}^{\mu\nu} = \frac{1}{2} \mathrm{Tr} \left[\not{k}' \gamma_\mu (1 - \gamma_5) \not{k} \gamma_\nu (1 - \gamma_5) \right]$$

$$\times \frac{1}{2} \mathrm{Tr} \left[(\not{p}' + M)\gamma^\mu (1 - \gamma_5)(\not{p} + M)\gamma^\nu (1 - \gamma_5) \right]. \tag{107}$$

Parton model in neutrino interactions

- Anticommuting the γ_5 matrix in the above trace the leptonic tensor is given as:

$$\text{Tr}\left[\not{k}'\gamma_\mu \not{k}\gamma_\nu(1-\gamma_5)\right] = 4\left[k'_\mu k_\nu + k'_\nu k_\mu - g_{\mu\nu}(kk') - i\epsilon_{\mu\nu\gamma\delta}k'^\gamma k^\delta\right], \tag{108}$$

where $\epsilon^{\mu\nu\alpha\beta}$ is *fully antisymmetric* tensor of rank four.

- Although the quark mass M is explicitly present in the expression for the corresponding quark tensor, it disappears once the trace in the quarkonic tensor is worked out:

$$\frac{1}{2}\text{Tr}\left[(\not{p}' + M)\gamma^\mu(1-\gamma_5)(\not{p} + M)\gamma^\nu(1-\gamma_5)\right] =$$

$$\text{Tr}\left[\not{p}'\gamma^\mu \not{p}\gamma^\nu(1-\gamma_5)\right] + \frac{M^2}{2}\underbrace{\text{Tr}\left[\gamma^\mu\gamma^\nu + \gamma^\mu\gamma_5\gamma^\nu\gamma_5\right]}_{0} \tag{109}$$

- N.B. Substituting $k \to p$, $k' \to p'$ we get exactly one half the result for the leptonic tensor.

Parton model in neutrino interactions

- Contracting the lepton and parton tensors using the identity

$$\epsilon_{\mu\nu\gamma\delta}\epsilon^{\mu\nu}_{\alpha\beta} = 2(g_{\alpha\delta}g_{\beta\gamma} - g_{\alpha\gamma}g_{\beta\delta}) \tag{110}$$

and employing standard Mandelstam variables for the parton level subprocess

$$s \equiv (k+p)^2, \quad t \equiv (k-k')^2 = (p-p')^2, \quad u \equiv (k-p')^2 = (k'-p)^2 \tag{111}$$

we get

$$L^{(1)}_{\mu\nu}L^{\mu\nu}_{(2)} = 32\left[(kp)^2 + (k'p)^2 + (kp)^2 - (k'p)^2\right] = 64(kp)^2 = 16\left(s - M^2\right)^2, \tag{112}$$

where the last two terms came from the contraction (110) and are therefore due to the presence of the γ_5 matrix.

- N.B. only this part may differ for particles and antiparticles. Switch to antiparticles, for both ν and q implies the substitutions $k \leftrightarrow k'$, $p \leftrightarrow p'$.
  $\Rightarrow$ Antisymmetry of term proportional to $\varepsilon_{\mu\nu\alpha\beta}$ means that it should be multiplied by -1 for each of these substitutions.

Parton model in neutrino interactions

This leads to two different situations:

1. Scattering of antineutrinos on antiquarks: As both of the mentioned substitutions are applied *simultaneously* we get exactly the same result as for the neutrino-quark channel.

2. Scattering of antineutrino on quark or neutrino on antiquark: here only one factor of -1 multiplies the term $(kp)^2 - (k'p)^2$ in (112) and we get

$$L_{\mu\nu}^{(1)}L_{(2)}^{\mu\nu} = 64(k'p)^2 = 16\left(u - M^2\right)^2 = 64(kp)^2(1-y)^2. \tag{113}$$

- N.B. Relation between (112) i.e.
  $L_{\mu\nu}^{(1)}L_{(2)}^{\mu\nu} = 32\left[(kp)^2 + (k'p)^2 + (kp)^2 - (k'p)^2\right] = 64(kp)^2 = 16\left(s - M^2\right)^2$
  and (113) is a particularly simple example of *crossing symmetry*. This symmetry relates the scattering amplitudes corresponding to the crossed channels of the basic $2 \to 2$ process (106) and holds under very general conditions even beyond the perturbation theory.

Parton model in neutrino interactions

- The y dependence can therefore be summarized as follows:

$$\frac{\mathrm{d}\sigma(\nu + q)}{\mathrm{d}y} = \frac{\mathrm{d}\sigma(\overline{\nu} + \overline{q})}{\mathrm{d}y} = \frac{G_F^2 s}{\pi}, \tag{114}$$

$$\frac{\mathrm{d}\sigma(\nu + \overline{q})}{\mathrm{d}y} = \frac{\mathrm{d}\sigma(\overline{\nu} + q)}{\mathrm{d}y} = \frac{G_F^2 s}{\pi}(1 - y)^2. \tag{115}$$

- Introducing all numerical factors we end up with the following expressions

$$\frac{\mathrm{d}\sigma^{\nu p}}{\mathrm{d}x\mathrm{d}y} = \frac{G_F^2 S x}{\pi} \left[(s(x) + d(x)) + (\overline{u}(x) + \overline{c}(x))(1 - y)^2 \right], \tag{116}$$

$$\frac{\mathrm{d}\sigma^{\overline{\nu} p}}{\mathrm{d}x\mathrm{d}y} = \frac{G_F^2 S x}{\pi} \left[(\overline{s}(x) + \overline{d}(x)) + (u(x) + c(x))(1 - y)^2 \right]. \tag{117}$$

Parton model in neutrino interactions

- In weak interactions parity is violated
  $\Rightarrow$ there are three independent structure functions in $\mathrm{d}\sigma/\mathrm{d}x\mathrm{d}y$ on a proton:

$$
\begin{aligned}
\frac{\mathrm{d}\sigma^{(\nu/\overline{\nu})\mathrm{p}}}{\mathrm{d}x\mathrm{d}y} &= \frac{G_F^2 S}{2\pi}\left[(1-y)F_2^{(\nu/\overline{\nu})\mathrm{p}} + 2x\frac{y^2}{2}F_1^{(\nu/\overline{\nu})\mathrm{p}} \pm y\left(1-\frac{y}{2}\right)xF_3^{(\nu/\overline{\nu})\mathrm{p}}\right] \\
&= \frac{G_F^2 S}{2\pi}\left[\left(\frac{1+(1-y)^2}{2}\right)F_2^{(\nu/\overline{\nu})\mathrm{p}} \pm \left(\frac{1-(1-y)^2}{2}\right)xF_3^{(\nu/\overline{\nu})\mathrm{p}}\right] (118)
\end{aligned}
$$

In second equality Callan-Gross relation $2xF_1 = F_2$ and was used.

- Comparing the above expression with QPM formulae (116) and (117) we find:

$$
\begin{aligned}
F_2^{\nu\mathrm{p}} &= 2x[s(x) + d(x) + \overline{u}(x) + \overline{c}(x)], & (119) \\
F_2^{\overline{\nu}\mathrm{p}} &= 2x[u(x) + c(x) + \overline{s}(x) + \overline{d}(x)], & (120) \\
xF_3^{\nu\mathrm{p}} &= 2x[s(x) + d(x) - \overline{u}(x) - \overline{c}(x)], & (121) \\
xF_3^{\overline{\nu}\mathrm{p}} &= 2x[u(x) + c(x) - \overline{s}(x) - \overline{d}(x)]. & (122)
\end{aligned}
$$

Parton model in neutrino interactions

- Particularly important are the combinations

$$\tfrac{1}{2}\left(F_2^{\overline{\nu}\mathrm{p}} - F_2^{\nu\mathrm{p}}\right) = x[(u-\overline{u})-(d-\overline{d})], \qquad (123)$$

$$
\begin{aligned}
\tfrac{1}{2}\left(F_2^{\nu\mathrm{p}} + F_2^{\overline{\nu}\mathrm{p}}\right) &= x(u+d+s+c+\overline{u}+\overline{d}+\overline{s}+\overline{c}) \\
&= x\Sigma(x) \doteq \tfrac{1}{2}\left(F_2^{\nu\mathrm{p}} + F_2^{\nu\mathrm{n}}\right) \equiv F_2^{\nu\mathrm{N}}, \qquad (124)
\end{aligned}
$$

$$
\begin{aligned}
\tfrac{1}{2}\left(F_3^{\nu\mathrm{p}} + F_3^{\overline{\nu}\mathrm{p}}\right) &= (u+d+s+c-\overline{u}-\overline{d}-\overline{s}-\overline{c}) \\
&= \Delta(x) \doteq \tfrac{1}{2}\left(F_3^{\nu\mathrm{p}} + F_3^{\nu\mathrm{n}}\right) \equiv F_3^{\nu\mathrm{N}}, \qquad (125)
\end{aligned}
$$

where the third equalities in the preceding two expressions are only approximate, neglecting small differences in sea quark distributions.

- For isoscalar targets F_2, F_3 can be experimentally determined from the following combinations:

$$F_2^{\nu\mathrm{N}} \sim \frac{\mathrm{d}\sigma^{\nu\mathrm{N}}}{\mathrm{d}x\mathrm{d}y} + \frac{\mathrm{d}\sigma^{\overline{\nu}\mathrm{N}}}{\mathrm{d}x\mathrm{d}y}, \qquad F_3^{\nu\mathrm{N}} \sim \frac{\mathrm{d}\sigma^{\nu\mathrm{N}}}{\mathrm{d}x\mathrm{d}y} - \frac{\mathrm{d}\sigma^{\overline{\nu}\mathrm{N}}}{\mathrm{d}x\mathrm{d}y}. \qquad (126)$$

Parton model in neutrino interactions

- Comparing (124) and (93) and neglecting in the latter term proportional to $k(x)$ (numerically very small) we get:

$$F_2^{\nu \mathrm{N}} \doteq \frac{18}{5} F_2^{\mathrm{eN}}, \qquad (127)$$

which expresses the **universality** of quark distribution functions in weak and electromagnetic interactions.

- Factor $\frac{18}{5}$ is a direct reflection of quark charges
  $\Rightarrow$ experimental confirmation of this relation, (Fig. 15), provides another evidence for their fractional values.
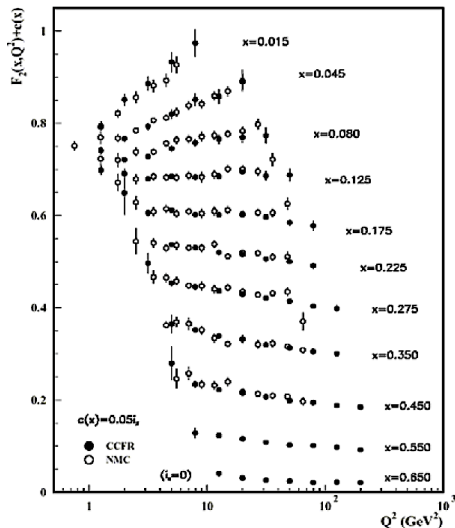
Figure 15: The comparison of $F_2^{\nu \mathrm{N}}(x, Q^2)$ and $(18/5) F_2^{\mathrm{eN}}(x, Q^2)$.

Parton model in neutrino interactions

- Fig. 15 also provides another argument against the Hahn-Nambu model of integral charge colored quarks which predicts $F_2^{\nu\mathrm{N}} = 2F_2^{e\mathrm{N}}$. Integrating $F_3^{\nu\mathrm{N}}(x, Q^2)$ over the whole kinematical range $x \in (0, 1)$ we get

$$\int_0^1 F_3^{\nu\mathrm{N}}(x, Q^2)\mathrm{d}x = \int_0^1 (u_v(x) + d_v(x))\mathrm{d}x, \qquad (128)$$

  which, according to the QPM, should be equal to 3, corresponding to the fact that there are two valence u quarks and one valence d quark in the proton.

- (128) is so called *Gross-Llewellyn-Smith sum rule* and has been tested experimentally with the result, $2.50 \pm 0.018(stat) \pm 0.078(syst)$, which deviates somewhat from the parton model prediction, but this deviation can be explained in QCD.

- Together with the sum rule (97) measuring the integral in (128) allows us to determine separately the integrals over $u_{val}(x)$ and $d_{val}(x)$, which provide a crucial bridge between the additive quark model and the parton model of Feynman.

Polarized nucleon structure functions

- Introduce *polarized quark distributions functions* $q_i\uparrow(x)$ ($q_i\downarrow(x)$) describing probability to find a quark of flavor i with a momentum fraction x and spin *parallel* (*antiparallel*) to the spin of the target nucleon.

- We assume $M_p = m_q = 0 \;\;\Rightarrow$ spin of p, q and $\bar{q}$ points along its momentum. For massless quarks the states with definite spin projections have also a definite handedness $\Rightarrow$ we can use (114)-(115) for ν.

- **Unpolarized** pdf are given as:
$$q_i(x) = q_i\uparrow(x) + q_i\downarrow(x), \;\; \bar{q}_i(x) = \bar{q}_i\uparrow(x) + \bar{q}_i\downarrow(x), \tag{129}$$

  while for **polarized** ones we also need the other combinations:
$$\Delta q_i(x) \equiv q_i\uparrow(x) - q_i\downarrow(x) + \bar{q}_i\uparrow(x) - \bar{q}_i\downarrow(x). \tag{130}$$

- The basic quantity is
$$\frac{\mathrm{d}\sigma\uparrow\downarrow}{\mathrm{d}x\mathrm{d}y} - \frac{\mathrm{d}\sigma\uparrow\uparrow}{\mathrm{d}x\mathrm{d}y} \tag{131}$$

  corresponding to parallel and antiparallel beam and target spin orientations, or better the asymmetry
$$A^{\mathrm{p}} \equiv \frac{\mathrm{d}\sigma\uparrow\downarrow - \mathrm{d}\sigma\uparrow\uparrow}{\mathrm{d}\sigma\uparrow\uparrow + \mathrm{d}\sigma\uparrow\downarrow}. \tag{132}$$

Polarized nucleon structure functions

- Using (114)-(115) it is straightforward to show that in QPM:

$$A^{\mathrm{p}}(x) = \frac{(1-(1-y)^2)\sum_i e_i^2 x \Delta q_i(x)}{(1+(1-y)^2)\sum_i e_i^2 x (q_i(x) + \overline{q}_i(x))}. \tag{133}$$

- **polarized structure function** of the proton $g_1^{\mathrm{p}}(x)$ is then given as:

$$g_1^{\mathrm{p}}(x) \equiv \frac{1}{2}\sum_i e_i^2 \Delta q_i(x) = \frac{A^{\mathrm{p}}(x)F_2(x)}{2xD(y)}, \quad D(y) \equiv \frac{1-(1-y)^2}{1+(1-y)^2}. \tag{134}$$

- Similarly for the neutron. The integrals

$$\Gamma_1^{\mathrm{p}} \equiv \int_0^1 \mathrm{d}x\, g_1^{\mathrm{p}}(x) = \frac{1}{2}\left(\frac{4}{9}\Delta(u) + \frac{1}{9}\Delta(d) + \frac{1}{9}\Delta(s)\right), \tag{135}$$

$$\Gamma_1^{\mathrm{n}} \equiv \int_0^1 \mathrm{d}x\, g_1^{\mathrm{n}}(x) = \frac{1}{2}\left(\frac{4}{9}\Delta(d) + \frac{1}{9}\Delta(u) + \frac{1}{9}\Delta(s)\right), \tag{136}$$

where $\Delta(q)$ stands for integrals over $\Delta q(x)$ and corresponds to $\Delta^P(q)$, have been measured in several experiments.

Polarized nucleon structure functions

- Results from SMC experiment at CERN where polarized 190 GeV μ collided with stationary target made of polarized p or d shown on Fig. 16 imply

$$\Gamma_1^{\mathrm{p}} = +0.136 \pm 0.011, \tag{137}$$

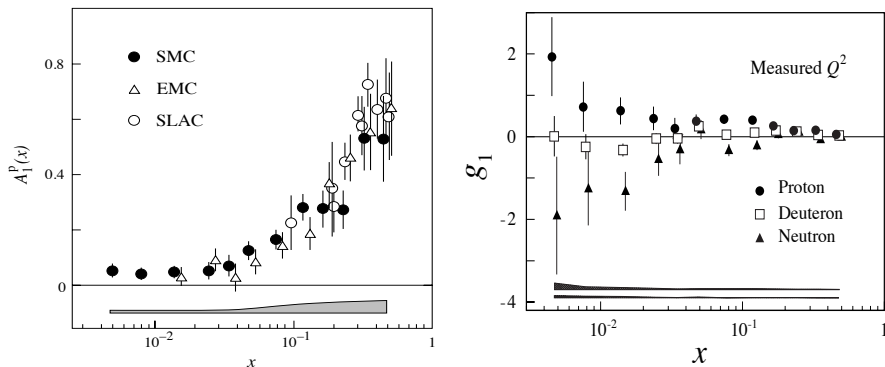$$\Gamma_1^{\mathrm{n}} = -0.063 \pm 0.024. \tag{138}$$

Figure 16: *Left:* spin asymmetry $A^{\mathrm{p}}(x)$. From SMC Collab.: Phys. Lett. B329 (1994), 399). *Right:* Polarized structure functions $g_1(x)$ for the proton (full circles), deuteron (open squares) and neutron (full triangles). From SMC Collab.: Phys.Rev.D56(1997)5330.

Polarized nucleon structure functions

- Increase of $A^p(x)$ as $x \to 1$ is primarily due to the vanishing of $F_2(x)$.
- Summing (137) and (138) we get

$$\Gamma_1^p + \Gamma_1^n = \frac{5}{18}\left(\Delta(u) + \Delta(d) + \frac{2}{5}\Delta(s)\right) = 0.073 \pm 0.03 \qquad (139)$$

and neglecting the strange content of the proton yields

$$\Delta(u) + \Delta(d) = 0.26 \pm 0.09, \qquad (140)$$

which gives the fraction of the spin of the proton carried by the u and d quarks and antiquarks.

- In a more rigorous treatment, where strange quarks are not neglected, we get

$$\Delta(u) = +0.82 \pm 0.04, \quad \Delta(d) = -0.44 \pm 0.04, \quad \Delta(s) = -0.11 \pm 0.04.$$
$$(141)$$

- The total contribution of quarks and antiquarks to the proton spin

$$\sum_q \Delta(q) \equiv \Delta(u) + \Delta(d) + \Delta(s) = 0.27 \pm 0.11 \qquad (142)$$

is still positive but small and the s quark contribution is significant.

Polarized nucleon structure functions

- The numbers (141) should be compared with the predictions

$$P_u^p(\Uparrow\uparrow) = \tfrac{5}{3}, \quad P_u^p(\Uparrow\downarrow) = \tfrac{1}{3}, \quad P_d^p(\Uparrow\uparrow) = \tfrac{1}{3}, \tag{143}$$

$$P_d^p(\Uparrow\downarrow) = \tfrac{2}{3} \Rightarrow \Delta^p(u) = \tfrac{4}{3}, \ \Delta^p(d) = -\tfrac{1}{3}, \tag{144}$$

  of the nonrelativistic quark model, where spins of the u and d constituent quarks add up to unity.

- In QPM this is not necessary the case and there are other possible carriers of the proton spin, like gluons and orbital momentum as well as other plausible explanations of the above results.

- Problem of what carries most of the proton spin represents one of the major puzzles of the present particle physics and remains the subject of intensive experimental as well as theoretical research.

Space–time picture of DIS and hadronization

Central QPM assumption – separation of a collision into two distinct stages:

1. The "hard" scattering of leptons on *individual* quarks.
   During this stage the influence of other partons in the nucleon is neglected and the cross–section of the lepton-parton subprocess calculated as if partons were as real as leptons. We thus disregard fact that the outgoing quark and remnant diquark cannot separate to infinity.

2. The "hadronization", i.e. that stage of the collision in which the outgoing quark and the proton remnant diquark convert into observable hadrons. This conversion is caused by the force acting between colored quarks as described in Section 3.11, which starts to be very strong when they are about 1 fm apart.

First stage is calculable within QPM. Description of second one is much more complicated. No real theory of hadronization – merely more or less sophisticated **models**.

Independent fragmentation model

- Was invented by Field and Feynman in the middle of seventies.
- The basic idea – hadronization of the outgoing quark-diquark system in Fig. 8 as an *independent* fragmentation of a quark and diquark.
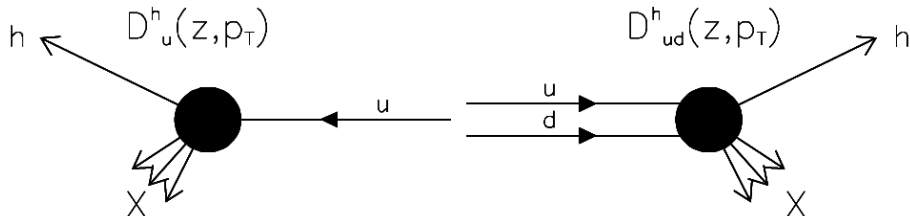- In IMF hadronization box of Fig. 8 is approximated as indicated in Fig. 17.

Figure 17: Hadronization of quark-diquark system, viewed in hadronic center of mass system. As they fly away, strong force, acting between them at distances larger than about 1 fm causes them to "radiate" hadrons. The big solid points represent the fragmentation functions.

Independent fragmentation model

- *Fragmentation function* (FF): $\qquad D_q^h(z, p_T),$ $\qquad\qquad\qquad$ (145)

  = probability that a parton q (quark, antiquark, diquark or gluon) produces ("fragments" into) a hadron h, carrying the fraction z of the original parton energy and the transverse (with respect to the direction of the fragmenting parton) momentum p_T.

- FFs are normalized as: $\qquad \sum_h \int_0^1 \int_0^\infty D_q^h(z, p_T)\mathrm{d}z\mathrm{d}p_T = \langle N_q \rangle,$ $\qquad$ (146)

  $\langle N_q \rangle$ = average multiplicity of hadrons coming from fragmentation of q.

- FFs are used, for instance, in **inclusive** production of hadrons in DIS,

$$\mathrm{e}^- + \mathrm{p} \to \mathrm{e}^- + h + \mathrm{anything} \qquad\qquad (147)$$

  i.e. when we are interested not only in the final state electron, but also of accompanying hadrons. However FF *don't* describe the *full* configuration of final state hadrons, as do modern event generators, like HERWIG or PYTHIA .

Independent fragmentation model

- Diff. cross-section of the process (147) is given as:

$$\frac{\mathrm{d}\sigma(ep \to e' + h + \text{anything})}{\mathrm{d}x\mathrm{d}y\mathrm{d}z\mathrm{d}p_T} = \frac{4\pi\alpha^2 S}{Q^4}\left(\frac{1 + (1-y)^2}{2}\right)\sum_i e_i^2 x q_i(x) D_{q_i}^h(z, p_T),$$

(148)

where the sum runs over all quarks inside the protons involved in the hard scattering with electron.

- Very often the p_T dependence of fragmentation functions is integrated over and one works with fragmentation functions $D_q^h(z)$ depending on the energy fraction z only. As the dependence on x and y in (148) *factorizes*, it is convenient to normalize it to $\mathrm{d}\sigma/\mathrm{d}x\mathrm{d}y$:

$$\frac{1}{\mathrm{d}\sigma/\mathrm{d}x\mathrm{d}y}\frac{\mathrm{d}\sigma(ep \to e' + h + \text{anything})}{\mathrm{d}x\mathrm{d}y\mathrm{d}z} = \frac{\sum_i e_i^2 q_i(x) D_{q_i}^h(z)}{\sum_i e_i^2 q_i(x)},$$

(149)

which is then *independent of y*.

- This quantity is also very suitable from experimental point of view as various systematical errors tend to cancel in the ratio (149).

Independent fragmentation model

- N.B. In neutrino interactions the x and y dependences *do not* factorize due to different y–dependences of quark and antiquark cross–sections and we thus get slightly more complicated relation:

$$\frac{1}{\mathrm{d}\sigma/(\mathrm{d}x\mathrm{d}y)} \frac{\mathrm{d}\sigma(\nu_\mu p \rightarrow \mu^- + h + \mathrm{anything})}{\mathrm{d}x\mathrm{d}y\mathrm{d}z} = \frac{d(x)D_u^h(z) + \bar{u}(x)(1-y)^2 D_{\bar{d}}^h(z)}{d(x) + \bar{u}(x)(1-y)^2}. \tag{150}$$

where only the light quarks u, d from the first generation and their antiquarks were taken into account.

- Basic feature of FF: the heavier the quark, the bigger the average fraction of its momentum, carried away by the meson, containing, as its valence quark, the fragmenting quark.

- We expect the following symmetry relations between different FFs:

$$D_u^{\pi^+} = D_d^{\pi^-} = D_{\bar{d}}^{\pi^+} = D_{\bar{u}}^{\pi^-}, \tag{151}$$

$$D_u^{\pi^-} = D_d^{\pi^+} = D_{\bar{d}}^{\pi^-} = D_{\bar{u}}^{\pi^+}, \tag{152}$$

$$D_s^{\pi^+} = D_s^{\pi^-} = D_{\bar{s}}^{\pi^+} = D_{\bar{s}}^{\pi^-}. \tag{153}$$

Parton model in other processes

- Both the parton distribution and fragmentation functions have been introduced to describe data on DIS. Neither of them can be calculated and must be determined from data.

- However, once they are extracted using data from one process[1], they can be used in any other one and thus allow nontrivial **predictions** to be made. This property of **universality** is the main benefit from QPM.

- We will now discuss several examples of other processes treated in QPM.
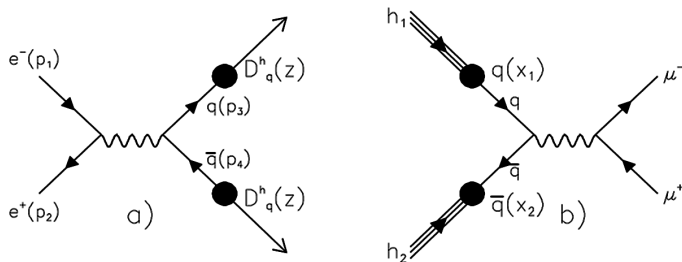
Figure 18: a) Lowest order Feynman diagram for the production of a $q\bar{q}$ pair in e^+e^- annihilation and its subsequent fragmentation in IFM; b) inverse process of dilepton pair production in hadronic collisions, via $q\bar{q}$ annihilation into a virtual photon. The big solid blobs stand in (a) for quark fragmentation functions and in (b) for quark distribution functions.

Electron-positron annihilations into hadrons

- First process to which the parton had been applied after its invention in early seventies. In the lowest order of QED it proceeds via the one photon annihilation into a parton-antiparton pair which subsequently converts into hadrons (hadronizes)

$$e^+ e^- \to q\overline{q} \to \text{hadrons.} \tag{154}$$

- Hadronization determines details of the final states in (154) but does not change the cross section of this process if we integrate over all possible hadron final states.

- Neglecting m_e but keeping that of the quark (m_q), the spin averaged matrix element squared $\mid \overline{M_{if}} \mid^2$ is:

$$\mid \overline{M_{if}} \mid^2 = \frac{e^4 e_q^2}{s^2} L_{\mu\nu}^{(1)}(p_1, p_2) L^{(2)\mu\nu}(p_3, p_4) = e^4 e_q^2 \left[a_T (1 + \cos^2 \vartheta) + a_L (1 - \cos^2 \vartheta) \right] \tag{155}$$

- The leptonic tensor $L_{\mu\nu}^{(1)}$ is given as in (28)

$$L_{\mu\nu}^{(1)}(p_1, p_2) \equiv \frac{1}{2} \mathrm{Tr} \left[\not{p_1} \gamma_\mu \ \not{p_2} \gamma_\nu \right] = 2 \left[p_{1\mu} p_{2\nu} + p_{1\nu} p_{2\mu} - g_{\mu\nu} (p_1 p_2) \right], \tag{156}$$

whereas its partonic counterpart $L^{(2)\mu\nu}$ depends on its spin.

Electron-positron annihilations into hadrons

- Working out the flux factor and final parton differentials we arrive at the following general expression for the differential cross section

$$\frac{\mathrm{d}\sigma}{\mathrm{d}\cos\vartheta^*} = \frac{\beta}{32\pi s} \mid \overline{M_{if}} \mid^2 = \frac{\pi\alpha^2 e_q^2 \beta}{2s} \left[a_T(1+\cos^2\vartheta^*) + a_L(1-\cos^2\vartheta^*) \right],$$
(157)

where $\beta = \sqrt{1-4m_q^2/s}$. Note that this threshold factor comes exclusively from kinematical considerations.

- Integrating the above expression over the scattering angle we get

$$\sigma_{tot} = \frac{\pi\alpha^2 e_q^2 \beta}{2s} \left[\frac{8}{3} a_T + \frac{4}{3} a_L \right].$$
(158)

Electron-positron annihilations into hadrons

- Taking into account that

partons with $s = \frac{1}{2} : L_{\mu\nu}^{(2)}(p_3, p_4) \equiv 2 \left[p_{4\mu} p_{3\nu} + p_{4\nu} p_{3\mu} - g_{\mu\nu}(p_4 p_3 + M_q^2) \right]$, (159)

partons with $s = 0 : L_{\mu\nu}^{(2)}(p_3, p_4) \equiv (p_3 - p_4)_\mu (p_3 - p_4)_\nu$, (160)

we find after straightforward contraction of leptonic and partonic tensors

$$\text{partons with } s = 1/2 \quad : \quad a_T = 1, \quad a_L = 1 - \beta^2, \quad (161)$$

$$\text{partons with } s = 0 \quad : \quad a_T = 0, \quad a_L = \beta^2. \quad (162)$$

- Summing over N_f quarks with spin $1/2$ in the region where $s \gg m_q^2$ we get

$$\sigma_{tot}(s, \mathrm{e^+e^-} \to \text{hadrons}) = \sum_{i=1}^{N_f} \sigma_{tot}(s, \mathrm{e^+e^-} \to \mathrm{q}_i \bar{\mathrm{q}}_i)$$

$$= \frac{4\pi\alpha^2}{3s} \sum_{i=1}^{N_f} \beta_i e_i^2 \xrightarrow[s \gg M_i^2]{} \frac{4\pi\alpha^2}{3s} \sum_{i=1}^{N_f} e_i^2. \quad (163)$$

Electron-positron annihilations into hadrons

- Normalizing (163) by cross-section for the production of a single $\mu^+\mu^-$ pair $4\pi\alpha^2/3s$, we obtain dimensionless quantity $R(s)$:

$$R(s) \equiv \frac{\sigma_{tot}(s, e^+e^- \to \text{hadrons})}{\sigma_{tot}(s, e^+e^- \to \mu^+\mu^-)} \xrightarrow[s \gg M_q^2]{} \sum_{i=1}^{N_f} e_i^2. \qquad (164)$$

- For scalar quarks $R(s)$ is given by the same expression except for the additional overall factor $1/2$.

- The above predictions can be tested in several ways.

  1. The simplest and clearest is measurement of (164). It doesn't need fragmentation functions and is thus *fully* calculable. Important ingredient, however, is **color** of quarks. In relations (163) or (164) it means simply multiplying their r.h.s. by a factor of 3.
  2. Another possibility is to look for the specific angular dependence (157) of outgoing quarks in the angular distribution of produced **hadrons**. As in the process of quark fragmentation hadrons are produced as **jets** of particles, collimated around the direction of the fragmenting quark, the angle of the latter can be reasonably accurately determined from the direction of these jets.
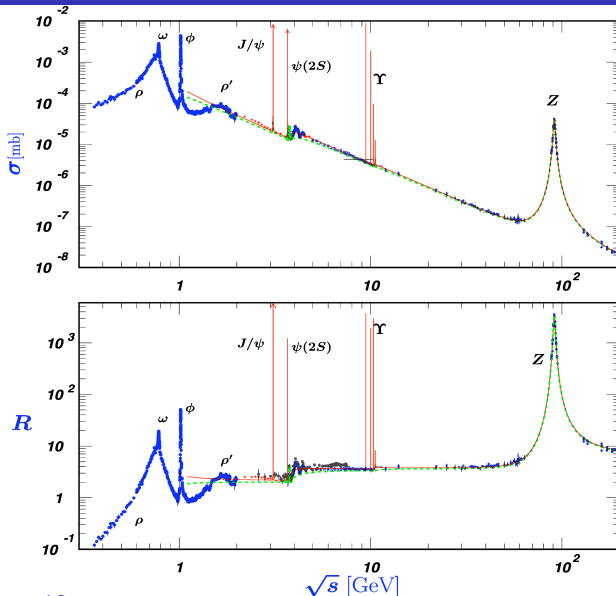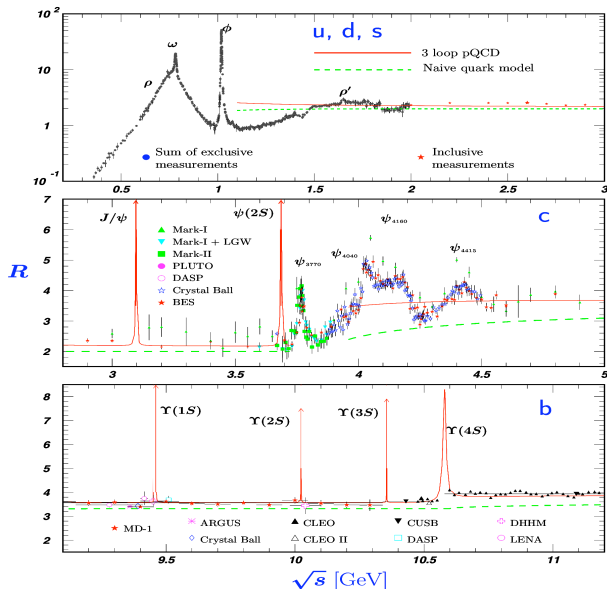
Figure 19: Broken green line – QPM, solid red line – pQCD. From PDG.

Figure 20: $R(s)$ in the light-flavor, charm, and beauty threshold regions. From PDG.

Tests of QPM in $e^+e^- \to q\overline{q} \to$ hadrons

- Comparing (164) to data in Figs. 19 and 20 shows that apart from the resonance structures, which the QPM clearly *cannot* reproduce, there would be also a *overall normalization factor problem* (about a factor 3.5) if the factor of 3 due to color of quarks was not used. Remaining discrepancy is explained as higher order QCD correction.

- Note that the Hahn-Nambu version of colored quarks predicts for the same quartet of quarks the value $R = 6$, and is thus definitely ruled out by the data.

- Parton fragmentation closely resembles particle showers in cosmic rays. The angular distribution of outgoing jets in the process (154) has been measured in a number of experiments and the expected form $(1 + \cos^2 \vartheta^*)$, predicted by the QPM for quarks with spin $1/2$, found in excellent agreement with data. This provides yet another evidence that quarks have spin $1/2$. For scalar quarks the angular distribution would be proportional to $(1 - \cos^2 \vartheta^*)$, which is clearly ruled out by the data.
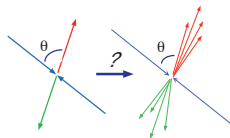

Figure 21: Parton to hadron transition for two jet events.

Figure 22: Two jet event in e^+e^- annihilation in OPAL detector at LEP.

- One can also study inclusive production of hadrons in the process

$$e^+e^- \to h + \text{anything} \qquad (165)$$

as a function of $z \equiv 2E^{(h)}/\sqrt{s}$. This process is described by the diagram in Fig. 18a, where FFs are represented by big solid blobs.

- Normalizing $d\sigma/dz$ by $\sigma_{tot}(e^+e^- \to \mu^+\mu-)$, the parton model predicts

$$\frac{1}{\sigma_{tot}(e^+e^- \to \mu^+\mu^-)}\frac{d\sigma}{dz} = \sum_i e_i^2 \left(D_i^h(z) + D_{\bar{i}}^h(z)\right). \qquad (166)$$

N.B. To make any sense FF should be independent of the process in which they are used. Experimentally this universality holds, indeed, very well.

- Notice the difference in shapes of fragmentation functions of light and heavy q into mesons containing them as valence quarks (see Fig. 23). The light quark FF are parameterized as:

$$D_q^h(z) = Az^a(1-z)^b(1+c/z), \qquad (167)$$

where A, a, b, c are free parameters, depending on the hadron h.

- FF of a heavy quark Q into a hadron containing this heavy quark is parameterized differently:

$$D_Q(z) = A \frac{z(1-z)^2}{\left((1-z)^2 + \varepsilon_Q z\right)^2}, \tag{168}$$

where the free parameter ε_Q, equal to 0.05 for the charm quark and 0.006 for the bottom one, determines the "hardness" of this fragmentation function.

- The weighted average over all quark fragmentation functions into pions as measured in e^+e^- annihilations by the TASSO Collaboration at DESY for four different primary energies are shown in Fig. 23a.

- The weak dependence of this fragmentation function on the primary energy, is of the same origin as the Q^2 dependence of the nucleon structure functions and can also be explained in QCD. The distribution of B-hadrons (i.e. mesons and baryons containing the bottom quark) as measured in e^+e^- annihilations at LEP and SLD for $\sqrt{s} = 91$ GeV is plotted in the upper right part of Fig. 23 in order to demonstrate the difference between the fragmentation functions of light and heavy quarks.
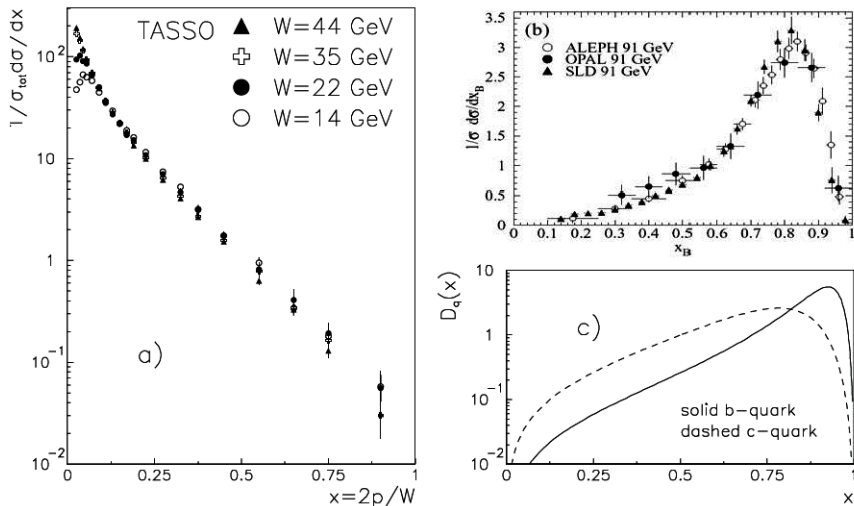
Figure 23: Measured fragmentation functions of light as well as heavy quarks into valence hadrons (hadrons containing the fragmenting quark) together with the analytical fits to fragmentation functions of heavy quarks c and b.

Drell-Yan production of heavy dilepton pairs

- The production of dilepton pairs in hadronic collisions

$$h_1 + h_2 \to \mu^+\mu^- + \text{anything} \qquad (169)$$

proceeds QPM via diagram in Fig. 18b.

]item $\mu^+\mu^-$ pair can be characterized by its mass m as well as the longitudinal and transverse (with respect to the collision axis) momenta $p_\parallel$ and p_T. Assuming h_1, h_2 collide head–on produced pair has no net transverse momentum p_T with respect to this (z-) axis. Instead of m and $p_\parallel$ it is convenient to introduce *dimensionless* variables

$$x_F \equiv \frac{2p_\parallel}{\sqrt{S}}; \quad \tau \equiv \frac{4m^2}{S}, \qquad (170)$$

where S stands for the square of the total CMS energy of colliding hadrons.

- Express x_F, τ in terms of the fractions $\overline{x}_1, \overline{x}_2$, carried by the annihilating quarks and antiquarks. Neglecting quark masses with respect to $\sqrt{S}$ we have

$$m^2 = x_1 x_2 S; \quad x_F = x_2 - x_1 \qquad (171)$$

where we have chosen the positive z-axis in the direction of the hadron h_2.

Drell-Yan production of heavy dilepton pairs

- Solving (171) for $\overline{x}_1, \overline{x}_2$ we find

$$\overline{x}_1 = \frac{1}{2}\left(-x_F + \sqrt{x_F^2 + \tau}\right), \tag{172}$$

$$\overline{x}_2 = \frac{1}{2}\left(+x_F + \sqrt{x_F^2 + \tau}\right). \tag{173}$$

- The differential cross section describing this process can be written as

$$\frac{\mathrm{d}\sigma}{\mathrm{d}m^2\mathrm{d}x_F} = \sum_i \int\int \mathrm{d}x_1\mathrm{d}x_2 q_i(x_1)\overline{q}_i(x_2)\delta(x_1 x_2 S - m^2)\delta(x_2 - x_1 - x_F)\underbrace{\left[\frac{4\pi\alpha^2 e_i^2}{3m^2}\right]}_{\sigma(m^2)}, \tag{174}$$

where the quark flavor index i in the above sum is understood to run over *both* quarks and antiquarks and the result (163) has been used (with the substitution $s \to m^2$) for $\mathrm{d}\sigma/\mathrm{d}m^2$.

Drell-Yan production of heavy dilepton pairs

- Integrating (174) over x_2 by means of the second δ-function we are left with the first δ-function in the form

$$\frac{1}{S}\delta(x_1^2 + x_1 x_F - \tau/4) = \frac{1}{S\sqrt{x_F^2 + \tau}}\delta(x_1 - \bar{x}_1) \quad \Rightarrow \quad (175)$$

$$\frac{m^3 \mathrm{d}\sigma}{\mathrm{d}m\mathrm{d}x_F} = \frac{8\pi\alpha^2}{3\sqrt{x_F^2 + \tau}}\left[\sum_i e_i^2 \bar{x}_1 q_i(\bar{x}_1)\bar{x}_2 \bar{q}_i(\bar{x}_2)\right]\frac{1}{3}, \quad (176)$$
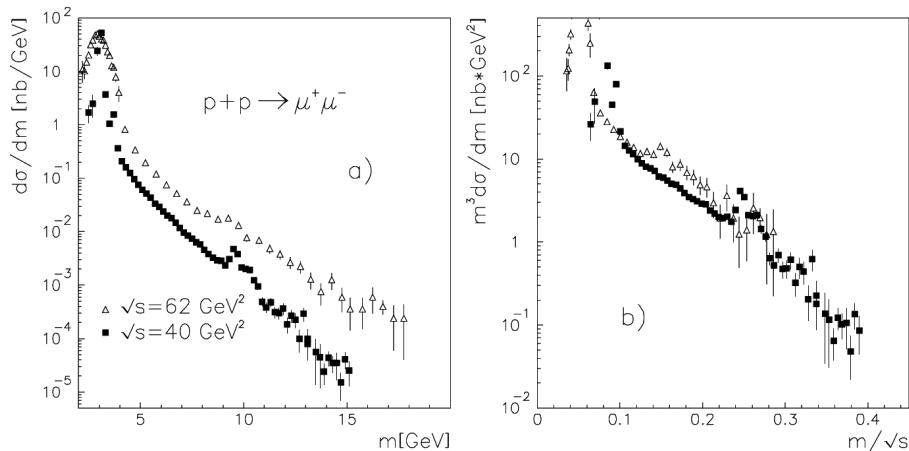
Drell-Yan production of heavy dilepton pairs

Figure 24: DY spectra as measured in pp collisions at CERN, ($\sqrt{s} = 62$ GeV) and Fermilab ($\sqrt{s} = 40$ GeV) displayed as a function of the dilepton mass m (a). In (b) the same spectra, but multiplied by m^3 and expressed as functions of $m/\sqrt{s}$ are compared, lending support to the QPM prediction of scaling (176)

Drell-Yan production of heavy dilepton pairs

Several aspects of the DY dilepton production are worth mentioning:

- The structures on Fig. 24 above the smooth DY continuum, described by the QPM model, correspond to the $c\bar{c}$ and $b\bar{b}$ bound states of the charmonium and bottomonium families. Experiments with protons, antiprotons and pions have demonstrated that for masses above roughly 3 GeV the QPM describes this continuum spectrum very well. For smaller masses the DY mechanism is clearly *below* the data.

- The quantity on the left hand side of (174) was defined in such a way that the r.h.s. of it depends on dimensionless variables x_F, τ only. So *independently* of the particular shape of quark distribution functions the QPM implies a nontrivial prediction by relating dilepton spectra at *different* energies, but the *same* τ. This is an analogue of the scaling phenomena in deep inelastic scattering of leptons on nucleons. Outside the resonance regions, the data plotted in Fig. 24b are in reasonable agreement with this basic prediction.

- The dilepton production in hadronic collisions (169), besides providing additional checks of basic QPM ideas, has also played a decisive role in the determination of quark distribution functions of **pions and kaons**, which are

Exercises

1. Carry out the contraction (30) in the laboratory frame and derive (34).

2. Perform explicitly the integration over δ-function in (31).

3. Calculate the scattering of electron on a charged scalar pointlike particle with electromagnetic coupling as defined in the text at the end of section 4.4.

4. Argue why the Mott cross section follows by replacing in the numerator of the Rutherford formula $m \to E$ and in its denominator $p \to E$.

5. Prove the so called Gordon decomposition

$$\overline{u}(p')\gamma_\mu u(p) = \overline{u}(p') \left[\frac{(p'+p)_\mu}{2m} + \mathrm{i}\frac{\sigma_{\mu\nu}}{2m}(p'-p)^\nu \right] u(p)$$

where $\sigma_{\mu\nu}$ is defined in (39) and m is the fermion mass.

6. Derive (39) exploiting gauge and Lorentz invariance and parity conservation.

7. Show that due to gauge invariance the value of elastic formfactor F_1 at $q^2 = 0$ is fixed: $F_1(0) = 1$.

Exercises

8. Show by nonrelativistic reduction of the Dirac equation that the value of κ in (39) gives the anomalous magnetic moment of the proton.

9. Derive the general form (45) for deep inelastic scattering using gauge and Lorentz invariance and parity conservation.

10. Show that for massless fermions the projection operator $(1 - \gamma_5)/2$ projects out states of particles with *negative* helicity (spin opposite to the momentum of the particle) and states of antiparticles with *positive* helicity (spin in the direction of momentum.

11. Calculate the angular distribution of scalar partons in e^+e^- annihilations as well as the magnitude of the integrated cross-section.

12. Evaluate the differential cross–section for the production of scalar quarks in e^+e^- annihilations. Compare the results on the angular dependence of the produced quarks as well as on the integrated cross–section with those of spin 1/2 quarks.

Figure 25: Low x data on $F_2^{\mathrm{ep}}(x, Q)$ as measured at HERA (H1 and ZEUS) and in fixed target experiments (BCDMS and E665).

In the small x region, roughly defined as $x \leq 10^{-2}$, theoretical description via the Altarelli–Parisi evolution equations encounters problems stemming from appearance of terms behaving typically as powers of $\ln(1/x)$. I shall not discuss theoretical ideas relevant for quantitative understanding of this region, but will merely show the latest experimental results from ep collider HERA at DESY.

Figure 26: Energy dependence of the total cross–section of real and virtual $\gamma^* p$ collisions.

In Fig. 25 the latest HERA data (H1 and ZEUS Collaborations) on $F_2^{\mathrm{ep}}(x, M)$ are shown together with the older fixed target data from muon–proton scattering at CERN (BCDMS and NMC) and at FERMILAB (E665). The rise of $F_2^{\mathrm{ep}}(x, M)$ at small x for all accessible values of Q^2 is

clearly visible. Taking into account the expression (75) the same data in small x region are replotted in Fig. 26 as the energy (i.e. W) dependence of the total cross–sections $\sigma(\gamma^*p; W, Q^2)$ for fixed Q^2. The figure includes also the data on total cross–section of real photon and indicates that the slope of the W–dependence of $\sigma(\gamma^*p; W, Q^2)$ increases with the photon virtuality Q^2. This feature is a source of intensive theoretical debate.